ANNALS OF PHYSICS 217, 105–141 (1992)

Landau Damping and Wall Dissipation in Large Metal Clusters

C. YANNOULEAS

Department of Physics, P. O. Box 2000, Virginia Commonwealth University, Richmond, Virginia 23284 and*
Istituto Nazionale di Fisica Nucleare, Sezione di Milano, Via Celoria 16, I-20133 Milan, Italy

AND

R. A. BROGLIA

Dipartimento di Fisica, Università di Milano, Via Celoria 16, I-20133 Milano, Italy, and Istituto Nazionale di Fisica Nucleare, Sezione di Milano, Via Celoria 16, I-20133 Milan, Italy, and The Niels Bohr Institute, DK-2100 Copenhagen Ø, Denmark

Received June 7, 1991

In analogy with nuclear many-body studies, the discrete-matrix random phase approximation (RPA) is used to describe the photoabsorption of large, spherical metal clusters. In this limit, the single-peak, classical Mie regime is valid and the matrix-RPA equations can be solved analytically. The RPA yields a closed formula for the width, Γ, of this peak due to Landau damping. This width is inversely proportional to the radius R of the cluster, in agreement with experimental observations for large silver and gold clusters embedded in a host medium. The RPA proportionality coefficient is unequivocally determined, and the reasons for the uncertainty in its value arising from disagreements among previous theoretical approaches are discussed. Specifically, $\Gamma = \lambda g(\hbar\Omega_{sp}/\varepsilon_F)\,\bar{v}/R$, where λ is the multipolarity of the plasma vibration, Ω_{sp} is the frequency of the surface plasmon, and ε_F is the Fermi energy of the conduction electrons. The function g varies from unity to zero as the frequency of the surface plasmon increases from zero to infinity. It is shown that the frequency dependence of g for a spherical shape is identical to that of a cubical boundary. $\bar{v} = (3v_F/4)\{1 + (\pi^2/6)(T/\varepsilon_F)^2\}$ is the average speed of a Fermi gas at temperature T. This result indicates a very small dependence on temperature, a trend in agreement with the observation.

A classical interpretation of this result is proposed based on the similarities with the one-body, wall-dissipation theory familiar from nuclear physics. According to this interpretation, the surface of the cluster is viewed as a moving wall whose interaction with the conduction electrons mimicks the multipole transitions induced by the electric field of the plasmon. This interpretation expresses Γ as the ratio, $\Gamma = \gamma/B$, of a surface friction coefficient, γ, over an inertia mass, B. The $1/R$ dependence results from the fact that the inertia mass is proportional to the volume, whereas the friction coefficient is proportional to the surface of the cluster.

* Present address.

0003-4916/92 $9.00

1. Introduction

1.1. *Optical Response of Large Metal Clusters*

The optical properties of metal clusters have been the focus of intense experimental [1–7] and theoretical investigations [8–22] in the last few years. The interest in this subject is due to the availability of mass-selected, free clusters that can be produced in molecular beams as a result of improved experimental techniques.

Yet, these experimental investigations are still in their early stages; they have been performed on the smallest mass numbers (40 atoms or less) and only for a limited number of metals (i.e., Na, K, and Cs). For these cases, theoretical calculations [10, 11, 20] based on the discrete-matrix RPA formalism—in the spirit of nuclear many-body approaches—have been successful in accounting for the experimental trends, and in particular, for the possibility of pronounced fragmentation of the surface plasmon, as well as for the redshift of its position with respect to the classical Mie theory [23].

Earlier experimental studies [24–30] of the optical response of metal clusters had been limited to large silver (or gold) clusters embedded in a supporting medium. Despite the fact that these samples were not mass-selected, but comprised a distribution of different mass sizes, these earlier investigations yielded valuable experimental information. Specifically, they showed that

1. the optical absorption spectrum of heavy metal clusters is dominated by a single peak in rough agreement with the classical Mie theory for the dipole excitation of a metal sphere;

2. the full width at half maximum, Γ, of this peak is almost temperature independent and inversely proportional to the radius, R, of the cluster.

Specifically, for the width, Γ, it was found that

$$\Gamma = A \frac{v_F}{R}, \tag{1}$$

where v_F is the Fermi velocity of the conduction electrons and A is a dimensionless constant of order unity.

A theoretical interpretation of this $1/R$ law was provided by Kawabata and Kubo [31] using a semiclassical linear-reponse approach for the imaginary part of the dielectric function of a metal sphere. Subsequent theoretical work [32–38] has reproduced the $1/R$ dependence, but there is no agreement (cf. Ref. [29]) concerning the precise value of the proportionality coefficient A. Comparison between theory and experiment has not been of particular assistance, since the host medium markedly influances [29] the value of the coefficient A.

On the other hand, the recently obtained results for free clusters indicate that the law (1) breaks down for very small sizes, as noticed in Ref. [4]. Indeed, Eq. (1) predicts for the small mass numbers (8 and 20 atoms) a much larger width than the

one actually observed. In this case, the broadening of the sharp RPA absorption lines is expected to result from the fluctuations of the surface of the system [17, 18, 22] and to exhibit an appreciable $\sqrt{T}$-temperature dependence.

Since the discrete-matrix RPA has successfully described the optical response of the smallest metal clusters, it is of considerable interest to inquire about its ability to account for the corresponding properties of the heavy, large clusters. This endeavor is of particular importance, since larger (up to 2000, and even higher, atoms), free, unsupported metal clusters have very recently become experimentally available [39, 40], providing for the first time the possibility to test the different theoretical predictions for the coefficient A.

It is the purpose of the present paper to show that the matrix-RPA formalism can indeed describe the optical response of the heavy metal clusters, and thus it can offer a unified theoretical framework for the whole range of masses, from the smallest to the the largest ones. Moreover, the correct value of the coefficient A will be derived for spherical clusters and for surface plasma oscillations of arbitrary multipolarity λ.

In particular, for a large spherical cluster, the plasmon width will be found in the present work to be given by

$$\Gamma_{\mathrm{RP}} = \lambda \frac{3}{4} \frac{v_{\mathrm{F}}}{R} g\left(\frac{\hbar \Omega_{\mathrm{sp}}}{\varepsilon_{\mathrm{F}}}\right), \tag{2}$$

where Ω_{sp} is the surface-plasmon frequency, ε_{F} is the Fermi energy, and $g(\zeta)$ is a frequency-dependent function that approaches unity as ζ approaches zero.

The present value $A = \frac{3}{4}$, for $\Omega_{\mathrm{sp}} = 0$ and $\lambda = 1$, is different from the corresponding value $A_{\mathrm{KK}} = 6/\pi^2$ [34] found by Kawabata and Kubo for a spherical particle. In addition, their function $g_{\mathrm{KK}}(\zeta)$ [34] decreases with the frequency faster than the corresponding function in Eq. (2). As a result, the Kawabata–Kubo expression noticeably underestimates the plasmon width compared to the present result. The discrepancy is due to the McMahon formula [41] for the location of the zeroes of a spherical Bessel function utilized in Ref. [31] (as well as in all other studies [35, 38] that considered the case of a spherical boundary). Namely, the McMahon formula yields a total density of states for a spherical Fermi gas that is lower than the actual one. In the present work, an improved expression for the number of the zeros of a spherical Bessel function has been used, and therefore the correct expression for the proportionality coefficient A has been determined.

1.2. *Connection with Nuclear Wall Dissipation*

The observed $1/R$ dependence of the broadening of the photoabsorption peak has been earlier [25] interpreted classically as the effect of diffuse, random collisions of the conduction electrons with the surface of the cluster. This interpretation leads to an effective mean free path, L_{eff}, for the conduction electrons, and to a width that is given by $v_{\mathrm{F}}/L_{\mathrm{eff}}$, in analogy with the usual theory of conductivity in the bulk

metal. For a sphere, $L_{\text{eff}} = R$ [42], and the constant A equals unity. As pointed out in Ref. [31], however, this interpretation is not satisfactory. The surface of the system cannot be considered as a fixed scatterer as if it were an impurity; it simply determines the single-particle states of the system. The decay of the plasmon is due to Landau damping induced by dipole transitions between these single-particle states.

The present work proposes a different classical interpretation. Instead of considering the surface as a fixed scatterer, it views it as a moving wall. The interaction of the moving wall with the conduction electrons mimics the dipole transitions and leads to a dissipative process known as wall dissipation. This interpretation does not need to invoke an effective, short mean free path that decreases along with the size of the cluster. On the contrary, this dissipative process is expected to be important for finite-size systems with a sharply demarcated boundary in the regime where the mean free path of the constituent fermions becomes larger than the dimensions of the system. This is the case, not only of atomic nuclei, but equally well of large metal clusters considered here.

The phenomenology of wall dissipation was introduced in nuclear physics by Swiatecki and coworkers [43] in order to model a dissipative dynamical approach to nuclear fission and heavy-ion collisions [44–46]. The connection of the nuclear wall dissipation with the microscopic RPA dynamics, and its ensuing interpretation as a special form of Landau damping, was later presented in Ref. [47] (cf. also Refs. [48, 49]).

The motivation for associating the broadening of the plasmon with the wall dissipation derives from the fact that $3v_F/4$ in the RPA result (2) is precisely the average speed, $\bar{v}$, of the particles of a Fermi gas at zero temperature. Indeed, according to the wall interpretation, the time-varying electric field associated with the surface plasmon creates an electric current and thus sets in motion, as a whole, the Fermi gas of the conduction electrons of the large cluster. There arises a velocity difference, $\mathbf{u}$, between the center-of-mass of the electron gas and the boundary of the cluster. In an equivalent way, one can think of the surface of the system as a rigid wall or piston moving with the opposite velocity, $-\mathbf{u}$, with respect to the Fermi gas. The ensuing energy dissipation rate, $\dot{E}_{\text{diss, wf}}(t)$, over the total surface area is given by the wall formula [43],

$$\dot{E}_{\text{diss, wf}}(t) = -\rho_\mu \bar{v} \oint u_n^2 \, dS, \tag{3}$$

where ρ_μ is the mass density and $\bar{v}$ is the average speed of the particles of the Fermi gas. Note that only the velocity component perpendicular to the surface enters into expression (3).

Small deformations of given multipolarity λ away from a spherical equilibrium shape of radius R are described with the help of the deformation variables α_λ, as

$$r = R + \alpha_\lambda \mathscr{Y}_{\lambda 0}(\theta), \tag{4}$$

and in such a case one finds for the energy dissipation rate over the total surface of the sphere,

$$\dot{E}_{\text{diss, wf}}(t) = -\rho_\mu \bar{v} R^2 \dot{\alpha}_\lambda{}^2 = -\gamma_{\text{wf}} \dot{\alpha}_\lambda{}^2. \tag{5}$$

Naturally, the friction coefficient γ_{wf} is proportional to the surface area. The width, Γ_{wf}, of the associated oscillatory motion is expressed [43, 50] as the ratio $\gamma_{\text{wf}}/B_\lambda$, where B_λ is usually taken to be the irrotational inertial mass of a Fermi droplet. This irrotational mass is proportional to the volume of the system. With respect to the deformation parameters α_λ, it is given [51] by

$$B_\lambda = \rho_\mu R^3/\lambda, \tag{6}$$

and hence one immediately derives that the classical width for a spherical particle is

$$\Gamma_{\text{wf}} = \lambda \frac{\bar{v}}{R}. \tag{7}$$

However, this width, Γ_{wf}, is precisely the RPA width, Γ_{RP}, of Eq. (2) in the case when $\hbar\Omega_{\text{sp}} \ll \varepsilon_{\text{F}}$.

1.3. *Plan of Paper*

The plan of the present paper is as follows:

- Section 2 reviews the formalism of the discrete-matrix RPA theory developed in nuclear physics [52, 53] and applied earlier in the case of very small metal clusters [10]. Subsequently, Section 2 describes the limiting case when the size of the cluster becomes large and derives an explicit microscopic expression for the width Γ_{RP} of the surface plasmon associated with Landau damping.
- Section 3 is devoted to describing the analytical integrations and to extracting the final, closed expression for Γ_{RP} under the simplifying assumption of an infinitely deep, spherical confining potential. This section also discusses the implications for the experiment, both concerning the dipole plasma mode in different metallic species and with respect to different multipole modes.
- Section 4 presents the classical model of wall dissipation and elaborates on the interpretation of the plasmon broadening in large clusters as the effect of this one-body/long-mean-free-path dissipative process. It also explains how the previously derived damping parameters for cubical geometries [34, 37] can be easily understood with the help of the wall-dissipation concept. Section 4 also presents the very small, but nonvanishing temperature contribution to the plasmon broadening that is consistent with the process of wall dissipation.
- Section 5 discusses in detail the reasons for the breaking down of the $1/R$ law

(cf. Eq. (1)) in the case of very small sizes, when the electronic single-particle states do not form a quasi-continuum of states but must be treated as individual discrete states.

• A general discussion concerning the universality of one-body dissipative processes (wall and window formulas [43]) for small systems and the prospect for their being relevant to fission and collisions of heavy metal clusters, in analogy with corresponding approaches in atomic nuclei, is presented in Section 6.

• The summary occupies Section 7.

• Appendix A contains the mathematical details that support the results presented in Section 3.

• Finally, Appendix B offers a detailed justification why expression (54) for the zeroes of a spherical Bessel function is the proper one to account for the correct total density of states of a spherical Fermi gas.

2. Large-Volume Limit of Discrete-Matrix RPA

2.1. *A Dispersion Relation for the Surface Plasmon and the Resulting Width from Landau Damping*

In the discrete-matrix RPA the exact physical, many-body eigenstates $|\nu\rangle$, are approximated with the solutions of the linearized equations of motion [52, 53] inside a particle–hole subspace, S, of finite dimensions. The RPA many-body wave functions in this subspace are given by

$$|\nu\rangle = Q_\nu^\dagger |0\rangle, \tag{8}$$

where $|0\rangle$ is the correlated ground state of the system and the RPA creation operator $Q_\nu^\dagger$ is a linear superposition of particle–hole excitations, i.e.,

$$Q_\nu^\dagger = \sum_{ph} \{X_{ph}(\omega_\nu)\, a_p^\dagger a_h - Y_{ph}(\omega_\nu)\, a_h^\dagger a_p\}. \tag{9}$$

Henceforth, the indices p, m, n will denote a particle, while the indices h, i, j will denote a hole. The amplitudes $X_{ph}(\omega_\nu)$, $Y_{ph}(\omega_\nu)$, and the eigenenergies $\hbar\omega_\nu$ determining the many-body states $|\nu>$ obey the RPA equations of motion

$$\begin{pmatrix} \mathscr{A} & \mathscr{B} \\ -\mathscr{B}^* & -\mathscr{A}^* \end{pmatrix} \begin{pmatrix} X(\omega_\nu) \\ Y(\omega_\nu) \end{pmatrix} = \hbar\omega_\nu \begin{pmatrix} X(\omega_\nu) \\ Y(\omega_\nu) \end{pmatrix}, \tag{10}$$

where the matrices $\mathscr{A}$ and $\mathscr{B}$ are specified by their elements as follows:

$$\mathscr{A}_{ph,\,p'h'} = \delta_{pp'}\,\delta_{hh'}(\varepsilon_p - \varepsilon_h) + V_{ph'hp'}; \qquad \mathscr{B}_{ph,\,p'h'} = V_{pp'hh'}. \tag{11}$$

Here $V_{\alpha\beta\gamma\delta}$ are the matrix elements of the residual two-body force and ε_α are the single-particle energies. In the case of small metal clusters, and in the framework of the local density approximation [54], this force is the Coulomb force slightly modified with additional contributions from exchange and correlation effects [8–10]. In the case of large clusters, however, the exchange-correlation contribution becomes negligibly small [15], and one needs to consider only the effect of the bare Coulomb force.

The system of Eqs. (10) is usually solved numerically, and then the distribution of the corresponding oscillator strengths for each eigenvalue $\hbar\omega_\nu$ is constructed; it determines the profile of the photoabsorption cross section. However, in many instances, and especially when among the states $|\nu\rangle$ there exists a prominent collective state, $|c\rangle$, carrying a large fraction of the total oscillator strength, it is helpful to divide the full problem in two steps. Following Ref. [55], we divide the full particle–hole space S in two parts, $S = S_R + S_A$; the first part—labeled as the restricted subspace, S_R—is responsible for building up the strong collective state $|c\rangle$, while the second part—labeled as the additional subspace, S_A—is responsible for the broadening of the collective peak.

In the case of large metal clusters, it is natural to construct the restricted subspace S_R from those particle–hole states with energies much smaller than the high energy, $\hbar\Omega_{sp}$, of the surface plasmon which agrees with the Mie resonance (for simple metals like Na and K, $\hbar\Omega_{sp} = \sqrt{\lambda/(2\lambda+1)}\,\hbar\omega_p$, where $\hbar\omega_p$ is the energy of the bulk plasmon). In particular, among other states, the subspace S_R comprises all the states of $\Delta N = 0$, 1, 2, 3 and 4 character, where $N = 2(n-1)+l$ is the principal single-particle quantum number. As explicitly shown by the numerical calculations [10, 11] (cf. also pp. 470 and 480 in Ref. [51]), these states with small ΔN carry most of the oscillator strength. In addition, unlike the case of the small clusters [10, 11, 20], where the $\Delta N = 3$ and $\Delta N = 4$ particle–hole states lie as high, and even higher, as the surface plasmon, the corresponding states in the large clusters lie much lower than the surface plasmon, and their energies become vanishingly small in the limit of very large volume. This behavior can be understood from a consideration of the evolution of the major shell of the equivalent harmonic oscillator. This quantity, which reflects the average distance between single-particle states decreases as $N_e^{-1/3}$, where N_e is the total number of free conduction electrons in the cluster.

The additional subspace S_A, responsible for the damping of the surface plasmon, consists of all those particle–hole states within a narrow energy band that are degenerate with the surface plasmon.

Taking into consideration this division into two subspaces, the original RPA excitation operator (9) and the RPA equations (10) are written as

$$Q_\nu^\dagger = \sum_{mi} \{X_{mi}(\omega_\nu)\, a_m^\dagger a_i - Y_{mi}(\omega_\nu)\, a_i^\dagger a_m\} + \sum_{\tilde{m}\tilde{i}} \{X_{\tilde{m}\tilde{i}}(\omega_\nu)\, a_{\tilde{m}}^\dagger a_{\tilde{i}} - Y_{\tilde{m}\tilde{i}}(\omega_\nu)\, a_{\tilde{i}}^\dagger a_{\tilde{m}}\}, \tag{12}$$

and

$$\begin{pmatrix} A & B & C & D \\ -B^* & -A^* & -D^* & -C^* \\ C & D & E & 0 \\ -D^* & -C^* & 0 & -E \end{pmatrix} \begin{pmatrix} X(\omega_\nu) \\ Y(\omega_\nu) \\ \tilde{X}(\omega_\nu) \\ \tilde{Y}(\omega_\nu) \end{pmatrix} = \hbar\omega_\nu \begin{pmatrix} X(\omega_\nu) \\ Y(\omega_\nu) \\ \tilde{X}(\omega_\nu) \\ \tilde{Y}(\omega_\nu) \end{pmatrix}, \tag{13}$$

where a tilde denotes quantities associated with the additional subspace S_A.

In Eq. (13), the submatrices A and B express the couplings among the states (m, i) of the restricted subspace, S_R, and have the form

$$A_{mi,nj} = \delta_{mn}\,\delta_{ij}(\varepsilon_m - \varepsilon_i) + V_{mjin}; \qquad B_{mi,nj} = V_{mnij}, \tag{14}$$

while the submatrices C and D describe the coupling between the subspaces S_R and S_A, and are given by

$$C_{mi,\tilde{n}\tilde{j}} = V_{mji\tilde{n}}; \qquad D_{mi,\tilde{n}\tilde{j}} = V_{mn\tilde{i}\tilde{j}}. \tag{15}$$

In writing Eq. (13), we assumed that the couplings among the states $(\tilde{m}, \tilde{\imath})$ of the additional subspace, S_A, can be neglected. As a result the matrix block

$$\begin{pmatrix} E & 0 \\ 0 & -E \end{pmatrix}, \tag{16}$$

is purely diagonal, and the submatrix E is of the form

$$E_{\tilde{m}\tilde{\imath},\tilde{n}\tilde{j}} = \delta_{\tilde{m}\tilde{n}}\,\delta_{\tilde{\imath}\tilde{j}}(\varepsilon_{\tilde{m}} - \varepsilon_{\tilde{\imath}}). \tag{17}$$

When the submatrices C and D are set equal to zero, the subspaces S_R and S_A decouple. Then the RPA equations within the restricted subspace S_R yield separate eigenenergies $\hbar\omega_\alpha$ and eigenvectors

$$\begin{pmatrix} x(\omega_\alpha) \\ y(\omega_\alpha) \end{pmatrix}. \tag{18}$$

Namely, the RPA equations within S_R are

$$\begin{pmatrix} A & B \\ -B^* & -A^* \end{pmatrix} \begin{pmatrix} x(\omega_\alpha) \\ y(\omega_\alpha) \end{pmatrix} = \hbar\omega_\alpha \begin{pmatrix} x(\omega_\alpha) \\ y(\omega_\alpha) \end{pmatrix}. \tag{19}$$

The index α here runs over the dimensions of the subspace S_R. Henceforth, we will assume that there is one highly coherent collective state $|c\rangle$ among the states $|\alpha\rangle$, which carries most of the total oscillator strength.

However, this collective state $|c\rangle$ is a sharp line without any broadening. The additional subspace S_A forms a quasicontinuum of states degenerate with the collective state. Due to the coupling between the subspaces S_R and S_A, the sharp

state $|c\rangle$ will broaden and acquire a finite width Γ. To derive a formula for this width in the case of a quasi-continuous S_A, it is more economical to introduce a time-dependent picture. This way, we will circumvent the mathematical subtleties for treating a pole in the stationary picture (cf. Refs. [55, 56]).

To introduce the time-dependent picture, we proceed as follows: In the total subspace, $S = S_A + S_A$, we consider time-evolving wave packets, $|\Phi(t)\rangle$, that are formed as a linear superposition of the RPA eigenstates $|v\rangle$. These wave packets can decay in time, unlike the stationary states $|v\rangle$, and are created by the action of a time-dependent operator $O^\dagger(t)$ on the correlated ground state, i.e.,

$$|\Phi(t)\rangle = O^\dagger(t)\,|0\rangle, \tag{20}$$

where

$$O^\dagger(t) = \sum_v b_v Q_v^\dagger\, e^{-i\omega_v t} = \sum_{ph} \{\Pi_{ph}(t)\, a_p^\dagger a_h - P_{ph}(t)\, a_h^\dagger a_p\}, \tag{21}$$

and the time-dependent amplitudes are given by

$$\Pi_{ph}(t) = \sum_v b_v X_{ph}(\omega_v)\, e^{-i\omega_v t} \tag{22}$$

and

$$P_{ph}(t) = \sum_v b_v Y_{ph}(\omega_v)\, e^{-i\omega_v t}. \tag{23}$$

Making the usual distinction between indices in the restricted and additional subspaces, the corresponding time-dependent RPA equations for the amplitudes $\Pi_{ph}(t)$ and $P_{ph}(t)$ have the form

$$\begin{pmatrix} A & B & C & D \\ -B^* & -A^* & -D^* & -C^* \\ C & D & E & 0 \\ -D^* & -C^* & 0 & -E \end{pmatrix} \begin{pmatrix} \Pi(t) \\ P(t) \\ \tilde{\Pi}(t) \\ \tilde{P}(t) \end{pmatrix} = i\hbar \frac{d}{dt} \begin{pmatrix} \Pi(t) \\ P(t) \\ \tilde{\Pi}(t) \\ \tilde{P}(t) \end{pmatrix}. \tag{24}$$

We now seek solutions of Eq. (24) of the form

$$\begin{pmatrix} \Pi(t) \\ P(t) \\ \tilde{\Pi}(t) \\ \tilde{P}(t) \end{pmatrix} = \begin{pmatrix} x(\omega_c) \\ y(\omega_c) \\ \tilde{\Pi}(\Omega) \\ \tilde{P}(\Omega) \end{pmatrix} e^{-i\Omega t + \eta t}, \tag{25}$$

where $\Omega \approx \omega_c - i\Gamma_{RP}/2$ is now a complex frequency. As a result, the time-dependent picture can describe a decaying time-evolution, unlike the stationary equations (13). Note that the substitution (25) is a shorthand notation, equivalent to Landau's

treatment [57] of going around the pole in the imaginary plane through appropriate Laplace transforms.

With the help of Eq. (19) and the RPA orthonormality relations, substitution of Eq. (25) into Eq. (24) and elimination of the amplitudes of the additional subspace yield the dispersion relation (for details, cf. Ref. [55, Appendix B])

$$\hbar\Omega - \hbar\omega_c + i\hbar\eta = \sum_{\tilde{m}\tilde{i}} \left\{ \frac{|K(\tilde{m}, \tilde{i}; \omega_c)|^2}{\hbar\Omega - \varepsilon_{\tilde{m}\tilde{i}} + i\hbar\eta} - \frac{|\Lambda(\tilde{m}, \tilde{i}; \omega_c)|^2}{\hbar\Omega + \varepsilon_{\tilde{m}\tilde{i}} + i\hbar\eta} \right\}, \tag{26}$$

where $\varepsilon_{\tilde{m}\tilde{i}} = \varepsilon_{\tilde{m}} - \varepsilon_{\tilde{i}}$, and the quantities $K(\tilde{m}, \tilde{i}; \omega_c)$ and $\Lambda(\tilde{m}, \tilde{i}; \omega_c)$ express the effective coupling between the collective state $|c\rangle$ and the states $(\tilde{m}, \tilde{i})$ of the additional subspace; they are given by

$$K(\tilde{m}, \tilde{i}; \omega_c) = \sum_{nj} \{ V_{\tilde{m}j\tilde{i}n} x_{nj}(\omega_c) + V_{\tilde{m}n\tilde{i}j} y_{nj}(\omega_c) \} \tag{27}$$

and

$$\Lambda(\tilde{m}, \tilde{i}; \omega_c) = \sum_{nj} \{ V_{\tilde{i}n\tilde{m}j} y_{nj}(\omega_c) + V_{\tilde{i}j\tilde{m}n} x_{nj}(\omega_c) \}. \tag{28}$$

Since the additional subspace forms a quasi-continuum, we can replace the summations with integrations. Then, with the help of the well-known formula

$$\lim_{\eta \to 0+} \frac{1}{x - e + i\eta} = \mathscr{P} \frac{1}{x - e} - i\pi\, \delta(x - e), \tag{29}$$

the dispersion relation (26) yields the following expression for the width Γ_{RP}

$$\Gamma_{\mathrm{RP}} = \frac{2\pi}{\hbar} \iint d\tilde{m}\, d\tilde{i}\, |K(\tilde{m}, \tilde{i}; \omega_c)|^2\, \delta(\hbar\omega_c - \varepsilon(\tilde{m}, \tilde{i})), \tag{30}$$

where the small modification of the real part ω_c of the collective frequency due to the principal value in (29) will be neglected henceforth.

Starting from the discrete-matrix RPA, we have derived a closed expression for the width Γ_{RP} of the surface plasmon in the case of large metal clusters. This expression is still fully microscopic but can be simplified by considering the average time-varying electric field of the surface plasmon. This simplification is carried out in the next subsection, where expression (30) is brought into complete equivalence with the linear-response expression of Kawabata and Kubo [31].

Before leaving this subsection, it should be observed that the present treatment of collective excitations of large metal clusters is quite analogous to the reversible Landau damping of bulk plasma oscillations as described by the many-body theory of ionized gases [57–59]. Besides reversibility, the analogy consists in that both the bulk plasmon mode and its decay by Landau damping are described by using the RPA approximation [58, 59]. However, the present treatment describes a finite

electron gas at zero temperature, whereas the original Landau-damping theory described an infinite electron gas at finite temperature [57].

2.2. *Simplifications Due to the Classical Field of the Surface Plasmon*

Expression (30) for the width of the surface plasmon is fully microscopic. Indeed, the effective coupling matrix element $K(\tilde{m}, \tilde{\imath}; \omega_c)$ is expressed through the two-body matrix elements $V_{\alpha\beta\gamma\delta}$ of the Coulomb force and the values of the forward-going and backward-going amplitudes $x(\omega_c)$ and $y(\omega_c)$. However, in the case of large clusters, a significant simplification can be achieved by noting that the effective matrix element $K(\tilde{m}, \tilde{\imath}; \omega_c)$ is simply the Fourier transform of the time-varying mean field associated with the collective state (cf. Ref. [60, especially Section 5]). Because of this property, one can try to guess appropriate approximations of the mean field and thus circumvent the full microscopic expression. In the case of a large metal cluster, where the regime of the single-peak Mie resonance is applicable, it is natural to approximate the mean field with the classical field of a metal sphere oscillating with multipolarity λ, namely to assume that

$$K(\tilde{m}, \tilde{\imath}; \omega_c) \sim \langle \tilde{m} | \, r^{\lambda} \mathscr{Y}_{\lambda 0}(\theta) \, | \tilde{\imath} \rangle. \tag{31}$$

This initial simplification leads to an additional one. As is familiar from nuclear physics [51–53], and as was suggested in Ref. [15] for the case of metal clusters, the result (31) of the simple multipole field can be effectively reproduced by replacing the Coulomb force by a separable two-body interaction of the form

$$V_{\alpha\beta\gamma\delta} = -\chi \, D^{\lambda}_{\alpha\gamma} \, D^{\lambda}_{\delta\beta}, \tag{32}$$

where

$$D^{\lambda}_{\alpha\gamma} = \langle \alpha | \, r^{\lambda} \mathscr{Y}_{\lambda 0}(\theta) \, | \gamma \rangle. \tag{33}$$

Naturally, away from the Mie regime, the radial dependence of the field is very different from the one in Eq. (31), and the multipole–multipole separable interaction is a poor approximation. This point was stressed in Ref. [20], were the case of the small sodium clusters Na_8, Na_{20}, and Na_{40} was considered. In that case, it was shown that the original, nonseparable Coulomb interaction was necessary to account for the pronounced fragmentation of the photoabsorption stength in several well-separated, distinct peaks.

With the assumption of the separable form for the two-body interaction, the Fourier transform of the time-varying part of the mean field becomes (cf. Eq. (27))

$$K(\tilde{m}, \tilde{\imath}; \omega_c) = n(\omega_c; \lambda) \langle \tilde{m} | \, r^{\lambda} \mathscr{Y}_{\lambda 0}(\theta) \, | \tilde{\imath} \rangle, \tag{34}$$

where the overall amplitude $n(\omega_c; \lambda)$ of the field is given by the expression

$$n(\omega_c; \lambda) = -\chi \sum_{nj} D^{\lambda}_{nj} \{ x_{nj}(\omega_c) + y_{nj}(\omega_c) \}. \tag{35}$$

This amplitude can be further calculated as follows: With the separable form (32), the RPA equations (19) in the restricted subspace can be solved for the amplitudes $x(\omega_c)$ and $y(\omega_c)$, and one obtains

$$x_{nj}(\omega_c) = \frac{n(\omega_c; \lambda)\, D^{\lambda}_{nj}}{\hbar\omega_c - \varepsilon_{nj}}; \qquad y_{nj}(\omega_c) = -\frac{n(\omega_c; \lambda)\, D^{\lambda}_{nj}}{\hbar\omega_c + \varepsilon_{nj}}. \tag{36}$$

The amplitudes $x(\omega_c)$ and $y(\omega_c)$ obey the RPA normalization

$$\sum_{nj} \{|x_{nj}(\omega_c)|^2 - |y_{nj}(\omega_c)|^2\} = 1. \tag{37}$$

This condition is sufficient to specify the amplitude $n(\omega_c; \lambda)$. Moreover, since the particle–hole excitations, ε_{nj}, in the restricted subspace are much smaller than the energy of the surface plasmon, we can expand the l.h.s. of Eq. (37) in powers of ε_{nj} and retain only the linear terms.

Then the energy-weighted sum rule

$$\sum_{nj} \varepsilon_{nj} |D^{\lambda}_{nj}|^2 = \frac{\lambda(2\lambda+1)}{4\pi} \frac{N_e}{2} \frac{\hbar^2}{\mu} \langle r^{2\lambda-2} \rangle, \tag{38}$$

can be invoked.

In the case of a uniform spherical density of radius R,

$$\langle r^{2\lambda-2} \rangle = \frac{3}{2\lambda+1} R^{2\lambda-2}, \tag{39}$$

and as a result the amplitude $n(\omega_c; \lambda)$ is found to be

$$n^2(\omega_c; \lambda) = \frac{\mu^2 \hbar \omega_c{}^3}{2\lambda^2} \frac{1}{B_\lambda R^{2\lambda-2}}. \tag{40}$$

In Eq. (40), B_λ is the irrotational inertial paramater defined in Eq. (6) of the Introduction.

Taking into consideration Eqs. (34) and (40), we can write expression (30) for the width Γ_{RP} as

$$\Gamma_{\mathrm{RP}} = \frac{\pi \mu^2 \omega_c{}^3}{\lambda^2} \frac{1}{B_\lambda R^{2\lambda-2}} \iint d\tilde{m}\, d\tilde{\imath}\, |D^{\lambda}_{\tilde{m}\tilde{\imath}}|^2\, \delta(\hbar\omega_c - \varepsilon(\tilde{m}, \tilde{\imath})). \tag{41}$$

A further simplification of Eq. (41) is achieved by noting that the matrix element $D^{\lambda}_{\tilde{m}\tilde{\imath}}$ can be written as a double commutator of the function $F(r, \theta) = r^{\lambda} \mathscr{Y}_{\lambda 0}(\theta)$ with the single-particle hamiltonian H_0, that is,

$$D^{\lambda}_{\tilde{m}\tilde{\imath}} = \frac{1}{\varepsilon^2_{\tilde{m}\tilde{\imath}}} \langle \tilde{m} | [H_0, [H_0, F]] | \tilde{\imath} \rangle, \tag{42}$$

where

$$H_0 = T + U(r) \tag{43}$$

is the static part of the single-particle hamiltonian; T is the kinetic-energy operator and $U(r)$ is the static average field that binds the valence electrons.

Using the property that

$$\nabla^2 F(r, \theta) = 0, \tag{44}$$

the double commutator in Eq. (42) is calculated to be

$$\begin{aligned}[H_0, [H_0, F]] &= -\left[H_0, \frac{\hbar^2}{\mu}\nabla F \cdot \nabla\right] \\ &= -\frac{\hbar^4}{\mu^2}\sum_{ij}(\partial_i \partial_j F)\,\partial_j \partial_i + \frac{\hbar^2}{\mu}\nabla F \cdot \nabla U,\end{aligned} \tag{45}$$

where the indices i and j sum over the cartesian coordinates.

For the case of a dipole field, the volume term (the first term) in the r.h.s. of Eq. (45) apparently vanishes. For a higher multipole, λ, it contributes mainly for particle–hole transformations of character $\Delta N \leqslant \lambda$, as can be estimated from a Fermi gas with a cubical boundary. Since the energies corresponding to these transitions decrease with increasing size of the cluster, this volume term can be neglected for the relevant transitions at the high energy of the surface plasmon (cf. also the Appendix of Ref. [35]).

As a result, we can retain only the surface term (second term) in the r.h.s. of Eq. (45), and find that

$$D^{\lambda}_{\tilde{m}\tilde{i}} \underset{R\to\infty}{=} \frac{\hbar^2}{\mu\varepsilon^2_{\tilde{m}\tilde{i}}}\langle \tilde{m}|\,\nabla F \cdot \nabla U\,|\tilde{i}\rangle, \tag{46}$$

In the case of large clusters, we can neglect the spill-out and assume that the profile of $U(r)$ is a spherical square well, i.e.,

$$U(r) = U_0\theta(r - R). \tag{47}$$

Explicitly introducing the multipole field in relation (46), we obtain for the matrix elements $D^{\lambda}_{\tilde{m}\tilde{i}}$,

$$D^{\lambda}_{\tilde{m}\tilde{i}} = \frac{\hbar^2}{\mu\varepsilon^2_{\tilde{m}\tilde{i}}}\lambda R^{\lambda-1}\langle \tilde{m}|\frac{dU}{dr}\mathscr{Y}_{\lambda 0}(\theta)\,|\tilde{i}\rangle. \tag{48}$$

Then taking into consideration the energy conservation imposed by the delta function, we derive the final expression for Γ_{RP}; it is of the form

$$\Gamma_{\mathrm{RP}} = \frac{1}{B_\lambda}\frac{\pi}{\omega_c}\iint d\tilde{m}\,d\tilde{i}\left|\langle \tilde{m}|\frac{dU}{dr}\mathscr{Y}_{\lambda 0}(\theta)\,|\tilde{i}\rangle\right|^2 \delta(\hbar\omega_c - \varepsilon(\tilde{m}, \tilde{i})) = \frac{\gamma_{\mathrm{RP}}}{B_\lambda}. \tag{49}$$

Naturally, in the case considered here, the collective state is the surface plasmon and $\omega_c = \Omega_{\mathrm{sp}}$. From Eq. (49), we see that the width of the surface plasmon for any

multipolarity λ is expressed as a surface effect through the derivative of the static mean field. It is also expressed as the ratio of a friction coefficient, γ_{RP}, over the irrotational mass, B_λ, in analogy with the classical view of a damped motion.

In the case of a dipole mode, expression (49) is fully equivalent to the linear-response expression for the real part, σ_1, of the effective conductivity derived by Kawabata and Kubo and given by Eq. (10) of Ref. [34]. To make the connection between effective conductivity and the width of the plasma mode, observe that $\Gamma = 4\pi\sigma_1\omega^2/\omega_p^2$, a relation that follows immediately from the Drude dielectric constant.

Furthermore, apart from a factor r resulting from a slightly different definition of the deformation parameter α_λ, the coefficient γ_{RP} in Eq. (49) agrees in detail with the quantal friction coefficient associated with the nuclear wall dissipation and given by Eq. (3.12) of Ref. [47]. This agreement is present in spite of the fact that the short-range, nuclear two-body force is very different from the long-range, Coulomb force.

Thus the Landau damping expressed by Eq. (49) is a feature of a universal dissipative regime appropriate for small Fermi systems. Here we summarize the conditions for its manifestation; they are:

1. the existence of a strong collective state carrying most of the oscillator strength;

2. that the volume of the system is large enough, so that the associated single-particle spectrum forms a quasi-continuum;

3. that the mean free path of the fermions is large compared to the dimensions of the system; then the RPA equations provide an adequate description and do not need to be modified by the addition of a two-body collision term.

The universality of the damping process described here is also reflected in the fact that the coupling constant χ does not enter into Eq. (49). Indeed, it is the precise value of χ that distinguishes among the separable interactions representing different two-body forces, e.g., nuclear forces from the Coulomb force. In the case of large metal clusters, the coupling constant χ is determined as follows:

Substitution of expressions (36) for the amplitudes $x(\omega_c)$ and $y(\omega_c)$ into Eq. (35) defining the field amplitude $n(\omega_c; \lambda)$ yields a dispersion relation for the frequency, Ω_{sp}, of the surface plasmon, namely,

$$2\sum_{nj}\frac{\varepsilon_{nj}\,|D_{nj}^{\lambda}|^2}{\hbar^2\Omega_{\mathrm{sp}}^2-\varepsilon_{nj}^2}=-\chi^{-1}. \tag{50}$$

Neglecting the particle–hole energies ε_{nj} in comparison with the plasmon energy, and using the sum rule (38), one finds (cf. also Ref. [15])

$$\chi^{-1}=-\frac{3(2\lambda+1)}{4\pi}\frac{N_{\mathrm{e}}}{\mu}\frac{R^{2\lambda-2}}{\omega_{\mathrm{p}}^2}, \tag{51}$$

where $\hbar\omega_{\mathrm{p}}$ is the energy of the bulk plasmon.

3. Evaluation of Surface-Plasmon Width (49)

3.1. *The Final Integrated Analytical Expression*

To derive the final formula for the width Γ_{RP}, we need to carry the integrations in Eq. (49). These integrations can be carried analytically under the assumption of an infinitely deep central potential, namely in the limit when $U_0 \to \infty$ (cf. Eq. (47)). This assumption has been also invoked in all the previous literature that produced a closed analytic expression [31–37]. However, apart from its expediency in producing closed analytical formulas, the assumption of an infinitely deep well expresses the physical properties of the actual self-consistent potential binding the valence electrons in the cluster—in spite of the finite depth of the latter. Indeed, the self-consistent potential for metal clusters has been calculated by various methods [61, 13]. When approximated by a finite square well, it is seen that these potentials are of the type utilized in nuclear physics to describe neutron resonances [62]; namely, even in the case of the smallest clusters, the binding-strength parameter $s = 2\mu U_0 R^2/\hbar^2$ is much larger than unity, i.e., $s \gg 1$. As a result, in the continuum range slightly above their rim where the surface plasmon lies, these potentials support sharp single-particle resonances embedded in the continuum, which may have a strong influence on the profile of the photoabsorption spectrum. In the case of small clusters, these resonances can be specified either by discretizing the continuum [10] or by a phase-shift analysis of the delocalized scattering states [63]. In the case of large clusters, the infinitely deep potential provides an economic way for isolating these resonances, which by this fact are shown solely responsible for the $1/R$ dependence of the width of the surface plasmon.

As mentioned earlier, the RPA friction coefficient, $\gamma_{RP} = B_\lambda \Gamma_{RP}$, was considered in Ref. [47], where its analytical integration was carried out. The calculation is straightforward, but lengthy, and the details are given in Appendix A. Here, we will highlight three pivotal points that guarantee an accurate final result. The second and third of these points differentiate the present approach from the calculation of Kawabata and Kubo [31], as well as from an earlier calculation by Lushnikov and Simonov [35] who utilized an RPA-propagator approach in the coordinate space.

Naturally, in the limit of an infinitely deep square well, the radial part of the single-particle wave functions is given by the spherical Bessel functions, $j_L(kr)$, and their vanishing on the boundary of the system provides the quantization condition

$$j_L(kR) = 0. \tag{52}$$

In the analytic evaluation, we first carry the integrations over the spatial variables, and then sum over the quantum numbers. Due to the delta function $\delta(r - R)$ arising from the derivative, dU/dr, of the step potential (47), the radial functions contribute only through their value at the surface, i.e., for $r = R$.

(i) Then the first point to be remembered is that the matrix elements in Eq. (49) can be evaluated analytically to be

$$\langle \tilde{m}| \frac{dU}{dr} \mathcal{Y}_{\lambda 0}(\theta) |\tilde{\imath}\rangle \underset{U_0 \to \infty}{=} \frac{\hbar^2}{\mu R} kk' \int \mathcal{Y}^*_{LM} \mathcal{Y}_{L'M'} \mathcal{Y}_{\lambda 0} \, d\Omega, \tag{53}$$

where the unprinted indices refer to the particle index $\tilde{m}$, while the primed indices refer to the hole index $\tilde{\imath}$.

(ii) The second important ingredient in the evaluation of Γ_{RP} is an appropriate expression for enumerating the single-particle states inside a spherical box.

We denote by n the number of single-particle radial eigenstates of wave number less than k for a given angular momentum (L, M). Thus n is equal to the number of zeroes of the spherical Bessel function $j_L(\rho)$ with $\rho = kr$ in the interval $0 < \rho \leqslant kR$. To carry the integrations over n the following expression for the density $dn/d\rho$ must be used:

$$\frac{dn}{d\rho}(L \text{ fixed}) \doteq \begin{cases} \dfrac{1}{\pi\rho}\sqrt{\rho^2 - L^2}, & \rho \geqslant L \\ 0, & \rho < L. \end{cases} \tag{54}$$

As shown in Appendix B, expression (54) yields the correct volume contribution for the density of states in a spherical box of large spatial volume. This volume contribution is independent of the shape of the box and thus equal to the result in the case of a cubic box. According to Ref. [64], it is also the leading term in an asymptotic expansion for the density of states and the only one surviving in the limit $k_{\mathrm{F}} R \to \infty$.

We note that expression (54) is essential in obtaining the correct result for the RPA width Γ_{RP}. Less accurate approximations for the number of zeroes do not suffice. In particular, the more familiar approximation,

$$dn \approx \frac{R}{\pi} dk, \tag{55}$$

which corresponds to the McMahon formula [41] for the zeroes of a Bessel function, as well as to the asymptotic expansion

$$j_L(kR) \sim \frac{1}{kR} \sin\left[kR - \frac{L\pi}{2}\right] \tag{56}$$

for the spherical Bessel functions, underestimates the correct result by a factor $6/\pi^2$. The reason for the deficiency of (55) is the fact that both the McMahon formula and the asymptotic form (56) are valid in the limit

$$L \ll \rho = kR. \tag{57}$$

This condition is always fulfilled in the case of scattering, but fails in the case of a spherical box. Indeed, in this latter case, the main contributions to the integrals come from values of L of the same order as $k_{\mathrm{F}} R$. One needs expressions for the

position of zeroes that hold when both the argument ρ as well as the order L are large (see Appendix B for details).

In the previous literature, and in particular in Ref. [31], the McMahon formula was used, and as result the width of the surface plasmon was underestimated, both through the lower value of $A_{KK}(\Omega_{sp}=0;\lambda=1)$ and through the faster decrease with frequency of the function $g_{KK}(\hbar\Omega_{sp}/\varepsilon_F)$.

(iii) The third important point is the summation over the angular momenta. It is precisely because of an oversight at this step that Ref. [35] found the value of $A_{LS}(\Omega_{sp}=0;\lambda)=(12\lambda)/(\pi(2\lambda+1))$ (cf. also Ref. [36]), which for $\lambda=1$ disagrees with the corresponding value of Kawabata and Kubo.

Specifically, by invoking the orthonormality relations of the Wigner 3-j symbols (cf. Appendix A), one can sum over the angular projections M and M', as well as over the angular momentum of the hole, L'. Namely, one effectively uses the identity

$$\sum_{M,M',L'}\left|\int \mathscr{Y}^*_{LM}\,\mathscr{Y}_{L'M'}\,\mathscr{Y}_{\lambda 0}\,d\Omega\right|^2=\frac{2L+1}{4\pi}. \tag{58}$$

As shown in Appendix A, consideration of the previous three important points yields the following intermediate expression (cf. Eq. (105)) for the friction coefficient γ_{RP} defined in Eq. (49):

$$\gamma_{RP}=\frac{\hbar k_F^4 R^2}{4\pi^2}\frac{2}{\zeta}\left[\int_0^{1-\zeta} dy\int_1^{1+\zeta} dz\,\sqrt{z-y}\,\sqrt{z-y-\zeta}\right.$$
$$\left.+\int_{1-\zeta}^{1} dy\int_{y+\zeta}^{1+\zeta} dz\,\sqrt{z-y}\,\sqrt{z-y-\zeta}\right],\qquad \zeta\leqslant 1, \tag{59}$$

where the dimensionless variables y and z are

$$y=(L/k_F R)^2,\qquad z=(\rho/k_F R)^2. \tag{60}$$

A corresponding equation holds for the case $\zeta>1$ and is given by Eq. (108) in Appendix A. Equations (59) and (108) show that the friction coefficient γ_{RP} is proportional to the surface area of the spherical cluster.

The final result for the friction coefficient γ_{RP} is given by Eqs. (107) and (108) in Appendix A as the dimensionless ratio γ_{RP}/γ_{wf}, where $\gamma_{wf}=\rho_\mu \bar{v}R^2=(\hbar k_F^4 R^2)/(4\pi^2)$ is the wall-formula friction coefficient (cf. Eq. (5)) when the spin degeneracy of the electrons is taken into account.

The expressions for γ_{RP}/γ_{wf} in Appendix A are lengthy, but they can be written in a compact form with the help of the inverse hyperbolic functions. Then using the relation $\Gamma_{RP}=\gamma_{RP}/B_\lambda$ and expression (6) for the irrotational mass (which is proportional to the volume), one finds the following final expression for the RPA width of the surface plasmon when $\lambda\ll k_F R$:

$$\Gamma_{RP}=\lambda\frac{3}{4}\frac{v_F}{R}\,g(\zeta), \tag{61}$$

where the function $g(\zeta)$ is of the form

$$g(\zeta)=\frac{1}{3\zeta}\{(1+\zeta)^{3/2}-(1-\zeta)^{3/2}\}+\frac{\zeta}{4}\{(1+\zeta)^{1/2}-(1-\zeta)^{1/2}\}$$
$$-\frac{\zeta}{4}(\zeta+2)\,\text{arc sinh}\left(\frac{1}{\sqrt{\zeta}}\right)-\frac{\zeta}{4}(\zeta-2)\left|\text{arc cosh}\left(\frac{1}{\sqrt{\zeta}}\right)\right|, \qquad \zeta\leqslant 1, \quad (62)$$

and

$$g(\zeta)=\frac{1}{3\zeta}(1+\zeta)^{3/2}+\frac{\zeta}{4}(1+\zeta)^{1/2}-\frac{\zeta}{4}(\zeta+2)\,\text{arc sinh}\left(\frac{1}{\sqrt{\zeta}}\right), \qquad \zeta>1, \quad (63)$$

with the dimensionless parameter ζ being the ratio of the surface-plasmon energy over the Fermi energy of the electron gas, namely,

$$\zeta=\frac{\hbar\Omega_{\text{sp}}}{\varepsilon_{\text{F}}}. \quad (64)$$

The function $g(\zeta)$ defined in Eqs. (62) and (63) was calculated for a *spherical* boundary. However, it agrees in detail with the corresponding functions derived in Refs. [32, 34, 37], but for a *cubical* boundary. In this respect, there is no difference between a spherical and a cubical boundary (and by analogy with any other boundary arbitrarily shaped, e.g., a cylinder), unlike the results listed in Refs. [34, 31]. The discrepancy is again due to the inaccuracy introduced by the McMahon prescription in counting the zeroes of the spherical Bessel function that was utilized in Refs. [34, 31]. This independent behavior of the function $g(\zeta)$ with respect to the shape of the boundary suggests that the energy-dissipation rate per unit area is the same for all shapes. The different values of the damping width, Γ_{RP}, between different shapes arise from purely geometrical factors, namely, from the different ratios of the surface versus the volume that are particular to each geometry.

3.2. *Implications for the Experiment*

The function $g(\zeta)$ is plotted in Fig. 1 and Fig. 2. Also in Fig. 2 the corresponding function $g_{\text{KK}}(\zeta)$ of Refs. [34, 31] is plotted to facilitate the comparison. It should be noted that $g(\zeta)$ starts from unity at $\zeta=0$ and decreases monotonically with increasing ζ. For $\zeta=1$ its value is $g(\zeta)=0.635$.

$g(\zeta)$ approaches zero as $\zeta\to\infty$. By expanding the inverse hyperbolic functions in powers of $\sqrt{1/\zeta}$, we find that the asymptotic behavior of $g(\zeta)$ is given by

$$\lim_{\zeta\to\infty} g(\zeta)=\frac{8}{15}\frac{1}{\zeta^{1/2}}+O\left(\frac{1}{\zeta^{3/2}}\right). \quad (65)$$

This frequency dependence of the width Γ_{RP} is expected to be reflected in the experimental observation. Moreover, the Fermi velocity of the electron gas depends on the Wigner–Seitz radius r_s of the metal, since $v_{\text{F}}=\hbar k_{\text{F}}/\mu$ and $k_{\text{F}}=(9\pi/4)^{1/3}(1/r_s)$.

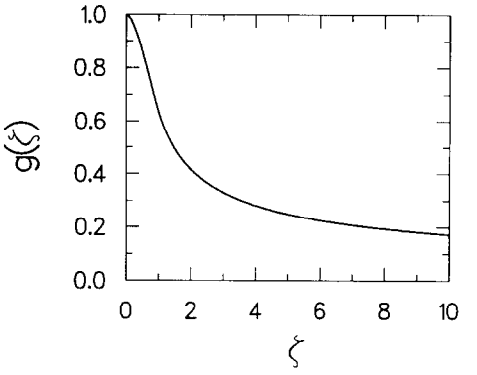

FIG. 1. The frequency-dependent RPA function $g(\zeta)$ for a spherical boundary (cf. Eqs. (62) and (63)). The dimensionless parameter ζ equals $\hbar\Omega_{sp}/\varepsilon_F$, where Ω_{sp} is the frequency of the surface plasmon and ε_F is the Fermi energy of the conduction electrons.

Taking into consideration that $\hbar^2/\mu = 2Ry \cdot bohr^2$ in atomic units, the overall dependence of the dipole width $\Gamma^{\lambda=1}_{RP,eV}$ on the Wigner–Seitz radius is given by the formula

$$\Gamma^{\lambda=1}_{RP,eV} = \frac{3}{2}\left(\frac{9\pi}{4}\right)^{1/3} g(\zeta_{\lambda=1}) \frac{13.6}{r_s R}\,\mathrm{eV} \cdot bohr^2$$

$$= 39.17\, g(\zeta_{\lambda=1}) \frac{1}{r_s R}\,\mathrm{eV} \cdot bohr^2. \tag{66}$$

The strong dependence of Γ_{RP} on the multipolarity λ is also remarkable. Indeed the width increases linearly with λ, and as a result higher multipolar surface plasmons will tend to overlap significantly. This seems to be consistent with the observation [65] in electron energy-loss-spectroscopy studies of small metallic spheres.

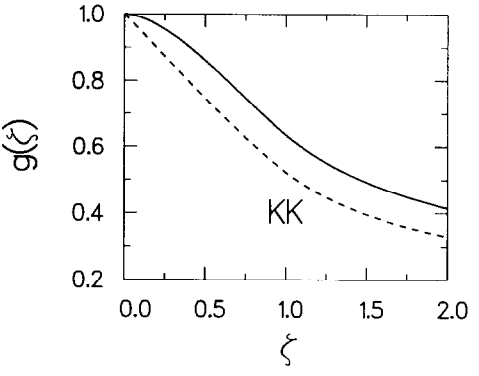

FIG. 2. The RPA function $g(\zeta)$ for a spherical boundary (solid line) compared to the corresponding function of Kawabata and Kubo (KK, dashed line) (cf. Refs. [34, 31]).

4. Classical Wall Dissipation and Temperature Dependence

4.1. *Wall Formula*

As was mentioned in the Introduction, one can interprete the broadening of the surface plasmon in large clusters as the effect of wall dissipation. The term wall dissipation refers to a classical analog that describes dissipative processes in the regime when the mean free path of the particles in a finite system is large compared to the dimensions of this system. The dissipative exchange of energy between collective and microscopic degrees of freedom may then be viewed as proceeding mainly through collisions of the particles with a moving boundary of the system (or, in a microscopic approach like the RPA, with the time-varying part of the mean field). This "one-body/long-mean-free-path" mechanism [43] contrasts with the "two-body/short-mean-free-path" dissipative mechanism of Navier–Stokes hydrodynamics, familiar from the case of ordinary liquids and gases.

For such a one-body dissipative process, we first seek a formula for the energy dissipation rate per unit area of the surface. Then the total dissipation rate, $\dot{E}_{\text{diss, wf}}$, is obtained by an integration over the total surface leading to the wall formula displayed in Eq. (3) of the Introduction.

To derive the wall formula, it is sufficient to consider a piston moving through a Fermi gas with velocity u. It is also convenient [66] to consider a frame of reference affixed to the moving piston. Then the total velocity distribution, f, for the Fermions is written as

$$f(v) = f_0(v^2 - 2vu\cos\theta) = f_0(v^2) + \delta f, \tag{67}$$

where f_0 is the velocity distribution of the Fermi gas in its own center-of-mass frame of reference, and the first-order change due to the motion of the piston is given by

$$\delta f = -2vu\cos\theta \frac{\partial f_0}{\partial v^2}. \tag{68}$$

In Eqs. (67) and (68), v is the particle velocity, u is the wall velocity, and θ is the angle between $\mathbf{v}$ and the z-axis which is taken parallel to $\mathbf{u}$ (cf. Fig. 3).

The first-order contribution, δP, to the pressure because of the motion of the piston is

$$\delta P = \frac{\rho_\mu}{\mu} \int_{-\infty}^{+\infty} \int_{-\infty}^{+\infty} \int_{-\infty}^{+\infty} F\,\delta f\, M\, dv_z\, dv_y\, dv_x, \tag{69}$$

where

$$F = v\cos\theta \tag{70}$$

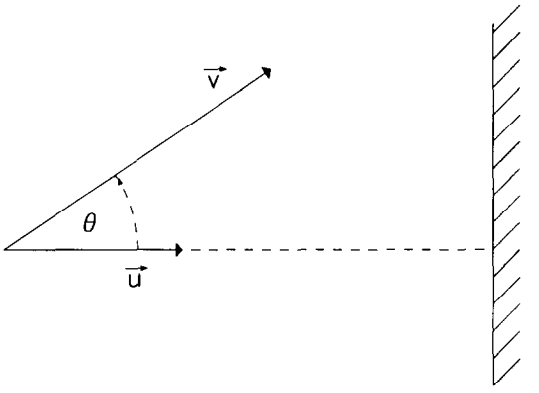

FIG. 3. Representation of particle velocity v and of wall velocity u when the frame of reference is affixed to the moving wall.

is the frequency per unit area of particle collisions with the wall for a given velocity, and

$$M = 2\mu v \cos\theta \tag{71}$$

gives the momentum transfer per collision; ρ_μ is the mass density of the gas and μ is the mass of the gas particles.

Substituting the corresponding quantities into Eq. (69) and using spherical coordinates, one obtains

$$\begin{aligned}\delta P &= \rho_\mu u \left\{4\int_0^{\pi/2} \cos^3\theta(-\sin\theta)\,d\theta\right\} \int_0^\infty 2\pi v^5 \frac{\partial f_0}{\partial v^2}\,dv \\ &= -\rho_\mu u \int_0^\infty \pi v^4\, df_0 = \rho_\mu u \int_0^\infty v(4\pi v^2)\, f_0(v^2)\,dv = \rho_\mu \bar{v} u,\end{aligned} \tag{72}$$

where $\bar{v}$ is the mean speed of the particles of the Fermi gas. In deriving (72), one carries an integration by parts and uses the assumption that $\partial f_0/\partial v^2$ falls rapidly enough to zero when $v^2 \to \infty$.

The wall-formula energy dissipation rate, $\dot{E}_{\text{diss, wf}}$, results from Eq. (72), when one multiplies with the wall velocity $-u$ and integrates over the total surface, i.e.,

$$\dot{E}_{\text{diss, wf}}(t) = -\rho_\mu \bar{v} \oint u_n^2\, dS. \tag{73}$$

Naturally, the integral over each differential element of the surface involves the perpendicular component of the velocity, u_n, to this surface.

It is instructive to apply the wall-dissipation model to the damping of the dipole

plasmon in a metallic particle shaped as a cube (or a film). In the case of a cubical boundary of length L, formula (73) yields

$$\dot{E}^c_{\text{diss, wf}}(t) = -\rho_\mu \bar{v}(2L^2)u^2 = -\gamma^c_{\text{wf}} u^2, \tag{74}$$

where the factor 2 in front of L^2 arises from the fact that only two faces are involved. Then, since the corresponding parameter B involves the total mass of the electrons, $B = \rho_\mu L^3$, and the width Γ^c equals

$$\Gamma^c = \frac{\gamma^c_{\text{wf}}}{B} = \frac{3}{2}\frac{v_F}{L}. \tag{75}$$

This is precisely the result for small values of Ω_{sp} found through a full quantum mechanical calculation in Refs. [32, 34, 37].

Certainly, the classical model cannot account for the frequency modification expressed by the functions (62) and (63). This modification is a purely quantum effect, and in this respect the classical wall-formula (73) for the energy dissipation rate needs to be generalized as follows:

$$\dot{E}_{\text{diss, wf}}(t) = -\rho_\mu \bar{v} g(\zeta) \oint u_n^2 \, dS. \tag{76}$$

4.2. *Temperature Dependence*

As discussed in Ref. [25], the experimental full width at half maximum (FWHM) of large silver clusters exhibits a very small temperature dependence. There are indications that this temperature contribution is also size dependent and varies as $1/R$.

The present theretical treatment of the RPA width Γ_{RP} allows for a straightforward incorporation of temperature effects in expressions (49) and (76). Indeed, in the case of a Fermi gas at finite, but small, temperature T, it is sufficient to consider that the average speed $\bar{v}$, which enters into these expressions, is given by

$$\begin{aligned}
\bar{v} &= \int \frac{d^3k}{(2\pi)^3}\frac{\hbar k}{\mu} F(\hbar k^2/2\mu; T) \Big/ \int \frac{d^3k}{(2\pi)^3} F(\hbar k^2/2\mu; T) \\
&= \frac{3}{4}\sqrt{\frac{2\eta}{\mu}}\left(1 + \frac{\pi^2}{3}\left(\frac{T}{\eta}\right)^2\right)\Big/\left(1 + \frac{\pi^2}{8}\left(\frac{T}{\eta}\right)^2\right) \\
&\approx \frac{3}{4}\sqrt{\frac{2\eta}{\mu}}\left(1 + \frac{5\pi^2}{24}\left(\frac{T}{\eta}\right)^2\right),
\end{aligned} \tag{77}$$

where $F(\varepsilon; T)$ here is the Fermi distribution at temperature T and η is the chemical potential at the same temperature. Since η depends on the temperature as

$$\eta \approx \varepsilon_F\left(1 - \frac{\pi^2}{12}\left(\frac{T}{\varepsilon_F}\right)^2\right), \tag{78}$$

the final expression for the average speed is of the form

$$\tilde{v} \approx \frac{3}{4} v_F \left(1 + \frac{\pi^2}{6} \left(\frac{T}{\varepsilon_F} \right)^2 \right). \tag{79}$$

In deriving Eq. (79), the Sommerfeld expansion [67] of $F(\varepsilon; T)$ has been used and only terms up to T^2 have been retained.

Since the Fermi energy of most metals is much larger than room temperatures, expression (79) indeed implies a very small temperature dependence for the width $\Gamma_{RP} = \lambda(\tilde{v}/R)\, g(\zeta)$. Practically, the RPA width Γ_{RP} is temperature independent. This behavior is particular to the Landau damping considered here and should be contrasted with the rather significant $\sqrt{T}$ dependence arising from the quadrupole fluctuations of the cluster surface, which is expected to be important in the case of very small clusters (cf. Refs. [17, 18, 11, 21]).

5. Breakdown of the $1/R$ Law in Small Clusters

The Landau-type RPA width (61) was derived under certain assumptions, namely,

1. that the spatial volume of the cluster is large enough so that the electronic single-particle spectra form a quasi-continuum. This allows the use in Eq. (30) of the delta function which expresses the conservation of energy between initial and final states;

2. that most of the oscillator strength resides in the immediate neighborhood of a single strong collective state, i.e., the Mie surface plasmon. This leads to replacing the residual Coulomb interaction with the effective multipole–multipole interaction (32).

These two assumptions are valid in the case of large clusters, but break down in the case of small clusters. In particular, the discreteness of the single-particle spectra cannot be ignored below a certain size. In the framework of the discrete-matrix RPA, this question was considered in Ref. [55] (cf. also Ref. [68]). Specifically, Ref. [55] found that, as long as the discrete additional particle–hole states are numerous enough, the strength of the single collective state, $|c\rangle$, will be distributed over the RPA states, $|\nu\rangle$, of the total subspace according to the probability

$$|f_{\nu c}|^2 = \frac{1}{1 + (\pi\kappa/d)^2 + (\hbar\omega_\nu - \hbar\omega_c)^2/\kappa^2}, \tag{80}$$

where d is the average spacing parameter for the particle–hole states in the additional subspace at energy $\hbar\omega_c$ and κ is a typical matrix element, $K(\tilde{m}, \tilde{\imath}; \omega_c)$, coupling the collective state $|c\rangle$ to these additional $1p$–$1h$ states (cf. Eq. (27)).

The RPA distribution (80) does not display, in general, the profile of a single broadened peak. However, when the subspace, S_A, of the additional particle–hole states is dense, namely when

$$(\kappa/d)^2 \gg 1. \tag{81}$$

the unity in the denominator of Eq. (80) can be neglected and the probability $|f_{vc}|^2$ acquires a Breit–Wigner form, i.e.,

$$|f_{vc}|^2 = \frac{d}{2\pi\hbar} \frac{\Gamma}{(\omega_v - \omega_c)^2 + (\Gamma/2)^2}, \tag{82}$$

which now exhibits a decay width Γ given by

$$\Gamma = \frac{2\pi}{\hbar} \frac{\kappa^2}{d}. \tag{83}$$

In the case of large clusters, $d \to 0$ and condition (81) is automatically fulfilled; as a result, the collective state is broadened due to Landau damping. Moreover, expression (83) for the FWHM can be replaced by the continuum expression (30) which leads to the $1/R$ law.

In the case of small clusters, however, the situation is totally different. Indeed, in the mass area of Na_{20}, one finds that the spacing parameter d is of the order of 0.7 eV. Additionally, the typical coupling matrix elements [20] are of the order of 0.1–0.4 eV, and thus condition (81) is no longer valid. The states of the additional subspace are not necessarily numerous enough, neither can they be treated as a quasi-continuum. As a result, the $1/R$ law for the Landau damping breaks down. In this case, the RPA fragments do not bunch together to form a single broadened peak as in Eq. (82). Instead, depending upon the individual cluster, detailed numerical calculations [10, 11, 20] using the full Coulomb interaction have shown that the RPA response may consist of one, two, or several strongly separated and well distinguishable sharp spikes that share the total oscillator strength. The experimentally observed broadening of these spikes is expected to come from the fluctuations of the cluster surface [17] and cannot be accounted for within the framework of the RPA. Unlike the case of large clusters, the breaking down of condition (81) in the case of small clusters results in photoabsorption profiles which not only are nontrivial compared to the prediction of the single Mie resonance, but are also highly dependent upon the individual cluster under consideration.

This different trend in the behavior between small and large clusters is illustrated in Fig. 4., where the distributions of oscillator strength for Na_{40} and Na_{1982}, according to the RPA numerical calculations are contrasted. In the case of Na_{1982} most of the strength fragments tend to group together within a narrow energy band of $\sim$0.1 eV around 3.4 eV. On the contrary, in the case of Na_{40}, the strength fragments are scattered over a wide energy range from 2.4 to 3.8 eV. When folded with Lorentzian curves in order to produce smooth shapes, the ensuing optical

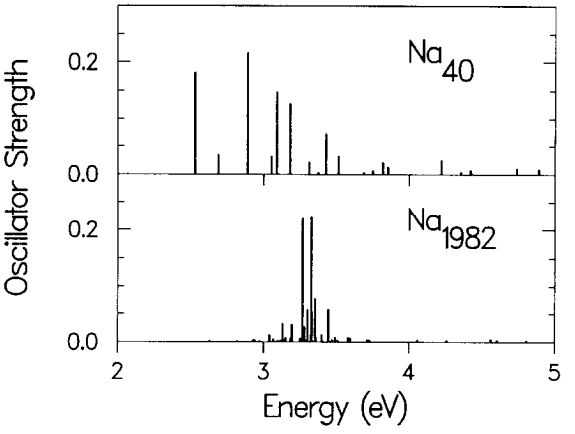

FIG. 4. Oscillator strengths for Na_{40} and Na_{1982} resulting from numerical RPA calculations with the full Coulomb force.

response of Na_{1982} would suggest a single peak, while the optical response of Na_{40} would exhibit a rather flat profile encompassing several well-separated peaks of comparable strength. In the former case, the corresponding full width at half maximum is in agreement with Eq. (66), while in the latter case it is much larger than the value resulting from the same expression.

It should be noted that the discreteness of the single-particle spectra is visible even in the case of 1982 sodium particle. As mentioned earlier, the smooth response observed experimentally results from additional broadening effects beyond the RPA. In the case of large clusters, the broadening introduced by these effects is smaller than the overall $1/R$ broadening of the Landau damping, and thus does not influence the value of the full width at half maximum.

A further example of the different behavior between small and large clusters is offered by the case of Na_8 [10]. Indeed, in spite of its mass proximity to Na_{40}, Na_8 exhibits one dominant peak with an experimentally determined width [2] of ~ 0.25 eV, which is now much smaller than the 0.7 eV predicted by Eq. (66). As noted in Ref. [4], K_9^+ and K_{21}^+, with 8 and 20 electrons respectively, exhibit one single peak that is much more narrow than the corresponding width from expression (66); hence they also belong to the same class of examples as does Na_8.

6. DISCUSSION: IMPLICATIONS FOR ISOSCALAR MODES

We have shown that the Landau damping of plasmons in large metal clusters can be viewed as a slowing down of the motion associated with the inertia of the conduction electrons due to the friction supplied by the wall formula. It is remarkable that this dissipative process is independent of the Coulomb force between the

electrons. Expressed as the energy dissipation rate per unit area, it only depends on the Fermi energy of the system. Thus it is not surprising that it was also derived for systems and modes very different than the fast plasma modes in metal clusters. In particular, the wall formula has also been derived in the case of slow shape vibrations of a large nucleus. These modes represent a shape distortion of the surface of the system in which the protons and neutrons move in phase. Such modes are called isoscalar in contradistinction to the isovector modes, like the giant dipole resonance, where the protons move against the neutrons (in this respect, the plasma modes in metal clusters belong to the class of isovector modes).

For a shape oscillation, whether in clusters or atomic nuclei, the time-varying part of the total mean field can be obtained (cf. p. 353 of [51]) by a deformation of the static potential. Then the appropriate separable two-body force is of the form

$$V_{\alpha\beta\gamma\delta} = \chi \langle \alpha | R \frac{dU}{dr} \mathscr{Y}_{\lambda 0}(\theta) | \gamma \rangle \langle \delta | R \frac{dU}{dr} \mathscr{Y}_{\lambda 0}(\theta) | \beta \rangle. \tag{84}$$

Since the final result is independent of the coupling strength χ, input of this force into the RPA equations leads again to the wall formula, as was shown in Ref. [47].

Shape vibrations in clusters are difficult to be directly observed due to the very small energies involved. Indeed in such a mode, the ionic cores will participate in the motion in order to keep in phase with the electrons, and as a result the inertia associated with this mode will increase by a factor of 1000 with respect to the case of plasma oscillations. However, as is the case with the atomic nuclei, the collective motion associated with the fission of clusters [69–72] or the collisions between them can be viewed as a straightforward extension of such shape modes. It is then natural to conjecture that frictional forces will play an important role in the dynamics of fissioning or colliding heavy metallic clusters. Unlike the nuclear case, however, such a possibility has not as yet been explored for metal clusters.

In the case of nuclei, these processes are treated within the framework of classical models which establish a balance between conservative, inertia, and dissipative terms governing the evolution of the collective motion. The wall formula is one of two members of a family of dissipative terms characterized as one-body dissipation. The other member is known as the window formula [43, 44] and is appropriate for two Fermi droplets with different velocities that come in contact through a small area during the collision process. The dissipation of the relative motion results from the transfer of particles from one droplet to the other and is, again, independent of the two-body force acting between the particles.

The approach of one-body dissipative dynamics has had a large effect on the theory of nuclear fission and deep inelastic heavy-ion collisions [45, 46]. As was discussed in Section 5, the limit of large volume provides the ideal regime for the unrestricted application of the wall formula; for small sizes, the shell structure inhibits the one-body dissipation. Fortunately, unlike the case of atomic nuclei, there is no upper limit in the number of constituent atoms in a cluster. Thus metal clusters appear to be an even more promising candidate than nuclei for the applica-

tion of one-body disipative dynamics, both for isovector modes, such as plasmons, as well as for isoscalar modes, such as shape vibrations, fission, and heavy-cluster collisions.

7. Summary

The nuclear, discrete-matrix version of RPA, earlier applied numerically to small clusters [10], was treated analytically to describe the response of large, spherical metal clusters. In particular, the RPA width Γ_{RP} of a surface plasmon of arbitrary multipolarity λ was specified by solving a dispersion relation, in anlogy with the original Landau-damping treatment [57] of the bulk plasmon in the infinite electron gas (cf. Section 2). Γ_{RP} was evaluated to be (cf. Section 3) frequency dependent and proportional to $1/R$, where R is the cluster radius. The RPA proportionality coefficient was unequivocally determined and is given for zero temperature by Eq. (61). The reasons for the earlier uncertainty in its value arising from disagreements [29] among previous theoretical approaches were discussed in detail. In particular, the inadequacy of the McMahon formula was stressed; for counting the numbers of zeroes of a spherical Bessel function, the present work utilized an improved expression (cf. Section 3), and thus the correct proportionality coefficient was determined. Specifically, for all plasmon frequencies, the present result for $\lambda = 1$ yields values noticeably higher than the corresponding result of Kawabata and Kubo [31]. In contrast to the previous litterature, the frequency dependence of Γ_{RP} for a spherical shape agrees precisely with the corresponding frequency dependence in the case of a cubical boundary. The correct value of the $1/R$ proportionality coefficient is of significant importance for the experiment, since free, unsupported heavy metal clusters have been recently produced in molecular beams [39, 40], unlike the large clusters which are embedded in a host medium and were used in earlier optical studies [29, 30]. These studies had shown that the host medium markedly affects the $1/R$ proportionality coefficient, and therefore the availability of free clusters offers for the first time the promise of isolating this influence.

The RPA result (61) for Γ_{RP} was found to be proportional to the average speed, $\bar{v}$, of the conduction electrons forming a Fermi gas, namely $\Gamma_{RP} \sim \bar{v}/R$. This fact led to a new classical interpretation of the $1/R$ broadening as the effect of a long-mean-free-path dissipative process known as wall dissipation (cf. Section 4) and widely studied in connection with the case of atomic nuclei [43, 47]. According to this view, the surface of the cluster can be considered as a moving wall whose interaction with the conduction electrons mimicks the multipole transitions induced by the field of the plasmon. Moreover, in analogy with the wall dissipation which is a surface effect, the RPA plasmon width is expressed as the ratio of a surface friction coefficient, γ_{RP}, over an irrotational mass, B_λ, proportional to the volume. Thus the $1/R$ dependence simply reflects the ratio of surface over volume. Expressed as per unit surface area, the corresponding energy dissipation rate at all frequencies is independent of the shape, a property that allows for an immediate calculation of the

plasmon width in the case of an arbitrary boundary. The different values of Γ_{RP} for various shapes result from the different ratios of the surface versus the volume.

The association of Γ_{RP} with the wall dissipation allows for a straightforward incorporation of finite-temperature effects. Indeed, it suffices to consider the temperature dependence of the average speed in a Fermi gas. This was done in Section 4, and the temperature dependence was found to be $1+(\pi^2/6)(T/\varepsilon_F)^2$, a result that indicates that Γ_{RP} is almost temperature insensitive.

The $1/R$ law is derived from the RPA only in the limit of a large cluster. In small clusters, shell effects and the discreteness of the spectra inhibit the process of wall dissipation. Section 5 discussed in detail the breakdown of the $1/R$ dependence for small sizes.

The wall dissipation exhibits a universal character; indeed, it is independent of the two-body force (the long-range Coulomb force in metal clusters or the short-range nuclear force) acting between the particles of the Fermi gas. In this respect, in addition to the fast isovector plasma modes, it is expected to be associated with other slower modes in metal clusters, in complete analogy with the nuclear case. Some implications of this universal behavior for the case of isoscalar modes in metal clusters—like shape vibrations, fission, and heavy-cluster collisions—were discussed in Section 6.

Appendix A

In this appendix, we calculate the coefficient γ_{RP} defined by Eq. (49) in the infinitely deep square-well potential/large-radius limit ($U_0 \to \infty$ and $R \to \infty$). To this end, we follow closely Ref. [47].

Because of assumption (47) that the shell-model potential is a spherical square well, and since $U_0 \to \infty$, all single-particle states are bound and have wave functions of the form

$$\psi(r, \theta, \phi) = C_L\, j_L(kr)\, \mathcal{Y}_{LM}(\theta, \phi), \qquad r \leqslant R, \tag{85}$$

where $j_L(kr)$ are the spherical Bessel functions, C_L is their normalization constant, and R is the radius of the spherical well.

Henceforth, we adopt the convention that unprimed indices denote a particle, while primed indices denote a hole, i.e.,

$$\tilde{m} \to (k_{Ln}, L, M), \qquad \tilde{\imath} \to (k_{L'n'}, L', M'), \tag{86}$$

where the wave numbers k_{Ln} and $k_{L'n'}$ take only those values which make the spherical Bessel function vanish at $r = R$, i.e.,

$$j_L(k_{Ln}R) = j_{L'}(k_{L'n'}R) = 0. \tag{87}$$

Then using the property that the derivative of the step function is a Dirac delta function, one obtains for the matrix elements in Eq. (49),

$$\langle \tilde{m}| \frac{dU}{dr} \mathcal{Y}_{\lambda 0}(\theta) |\tilde{\imath}\rangle = U_0 R^2 C_{Ln} C_{L'n'} j_L(k_{Ln}R)\, j_{L'}(k_{L'n'}R) \int \mathcal{Y}^*_{LM}\, \mathcal{Y}_{L'M'}\, \mathcal{Y}_{\lambda 0}\, d\Omega. \tag{88}$$

The integral over the three spherical harmonics imposes the conservation of parity and angular momentum on the plasmon–electron scattering, and for low plasmon multipolarity λ it requires that L and L' be of nearly the same magnitude.

To calculate the normalization constant, we use the orthogonality integral for the spherical Bessel functions [73], namely

$$C_{Ln}^{-2} = \int_0^R j_L(k_{Ln}r)\, j_L(k_{Ln'}r)\, r^2\, dr = \frac{R^3}{2} [j_{L+1}(k_{Ln}R)]^2\, \delta_{nn'}, \tag{89}$$

where k_{Ln} and $k_{Ln'}$ are two values satisfying the vanishing of the wave functions at the boundary.

Because of the continuity condition at the boundary satisfied by the wave functions, the following limit holds when $U_0 \to \infty$:

$$\lim_{U_0 \to \infty} \sqrt{2\mu U_0/\hbar^2}\, j_L(k_{Ln}R) = -\frac{dj_L(k_{Ln}r)}{dr}\bigg|_{r=R} = -k_{Ln} \frac{dj_L(\rho)}{d\rho}\bigg|_{\rho = k_{Ln}R}. \tag{90}$$

One can relate the normalization constant (89) to expression (90) with the help of the vanishing of the eigenfunctions at the spherical surface and of the recurrence relations of the spherical Bessel functions [73], namely,

$$\begin{aligned} j_{L-1}(\rho) + j_{L+1}(\rho) &= \frac{2L+1}{\rho}\, j_L(\rho), \\ L j_{L-1}(\rho) - (L+1) j_{L+1}(\rho) &= (2L+1) \frac{dj_L(\rho)}{d\rho}. \end{aligned} \tag{91}$$

Combining Eqs. (89), (90), and (91), one finds

$$\langle \tilde{m}| \frac{dU}{dr} \mathcal{Y}_{\lambda 0}(\theta) |\tilde{\imath}\rangle \underset{U_0 \to \infty}{=} \frac{\hbar^2}{\mu R} k_{Ln} k_{L'n'} \int \mathcal{Y}^*_{LM}\, \mathcal{Y}_{L'M'}\, \mathcal{Y}_{\lambda 0}\, d\Omega. \tag{92}$$

Substituting (92) into Eq. (49), one obtains

$$\gamma_{\mathrm{RP}} = \frac{2\pi\hbar^4}{\mu^2 \omega_c R^2} \sum_{LL'} \iint dn\, dn' (k_{Ln} k_{L'n'})^2 \sum_{MM'} |\mathcal{Y}^*_{LM}\, \mathcal{Y}_{L'M'}\, \mathcal{Y}_{\lambda 0}\, d\Omega|^2\, \delta(\hbar\omega_c - \varepsilon(\tilde{m}, \tilde{\imath})). \tag{93}$$

The overall factor of 2 accounts for the spin degeneracy . The number n (n') denotes the number of single-particle radial eigenstates of wave number less than k_{Ln} ($k_{L'n'}$) inside the spherical box for a given angular momentum (L, M)

$((L', M'))$. Thus n is equal to the number of zeroes of the spherical Bessel function $j_L(kr)$ in the interval $0 \leqslant r \leqslant R$.

The sum over indices M and M' is calculated with the help of the relations of the Wigner 3-j symbols [74]:

$$\int \mathcal{Y}_{L,-M}\, \mathcal{Y}_{L',M}\, \mathcal{Y}_{\lambda 0}\, d\Omega = \left[\frac{(2\lambda+1)(2L+1)(2L'+1)}{4\pi}\right]^{1/2} \begin{pmatrix} L & L' & \lambda \\ 0 & 0 & 0 \end{pmatrix} \begin{pmatrix} L & L' & \lambda \\ -M & M & 0 \end{pmatrix}, \tag{94}$$

$$\sum_{m_1 m_2} \begin{pmatrix} j_1 & j_2 & j_3 \\ m_1 & m_2 & m_3 \end{pmatrix} \begin{pmatrix} j_1 & j_2 & j_3' \\ m_1 & m_2 & m_3' \end{pmatrix} = (2j_3+1)^{-1}\, \delta_{j_3 j_3'}\, \delta_{m_3 m_3'}\, \delta(j_1 j_2 j_3), \tag{95}$$

where $\delta(j_1 j_2 j_3) = 1$ if j_1, j_2, j_3 satisfy the triangular condition and is zero otherwise.

Using Eqs. (94) and (95), one finds

$$\begin{aligned} \sum_M \left| \int \mathcal{Y}_{L,-M}\, \mathcal{Y}_{L',M}\, \mathcal{Y}_{\lambda 0}\, d\Omega \right|^2 &= \frac{(2\lambda+1)(2L+1)(2L'+1)}{4\pi} \begin{pmatrix} L & L' & \lambda \\ 0 & 0 & 0 \end{pmatrix}^2 \sum_M \begin{pmatrix} L & L' & \lambda \\ -M & M & 0 \end{pmatrix}^2 \\ &= \frac{(2L+1)(2L'+1)}{4\pi} \begin{pmatrix} L & L' & \lambda \\ 0 & 0 & 0 \end{pmatrix}^2 \delta(LL'\lambda). \end{aligned} \tag{96}$$

The particle–hole energy $\varepsilon(\tilde{m}, \tilde{\imath})$ is equal to

$$\varepsilon(\tilde{m}, \tilde{\imath}) = \frac{\hbar^2}{2\mu}(k_{Ln}^2 - k_{L'n'}^2) = \frac{\hbar^2}{2\mu R^2}(\rho^2 - \rho'^2), \tag{97}$$

where the dimensionless variables $\rho = k_{Ln} R$ and $\rho' = k_{L'n'} R$ have been introduced; they lie within the ranges

$$\begin{aligned} 0 \leqslant \rho' \leqslant k_F R \qquad & \text{(for a hole)}, \\ k_F R \leqslant \rho < \infty \qquad & \text{(for a particle)}, \end{aligned} \tag{98}$$

where k_F is the Fermi wave number.

For the density $dn/d\rho$ of the zeros of a spherical Bessel function $j_L(\rho)$ with given L, we use expression (54). The leading-order contribution to the integral of (93) results from values of L and L' large compared to λ ($\ll k_F R$). Then L and L' are nearly equal so that

$$\frac{dn'}{d\rho'} = \frac{1}{\pi\rho'}\sqrt{\rho'^2 - L'^2} \approx \frac{1}{\pi\rho'}\sqrt{\rho'^2 - L^2}. \tag{99}$$

With Eqs. (99) and (96), Eq. (93) yields

$$\gamma_{RP} = \frac{\hbar^4}{2\pi^2\mu^2\omega_c R^6} \sum_L \iint d\rho\, d\rho'(\rho\rho') \sqrt{\rho^2 - L^2}\sqrt{\rho'^2 - L^2}(2L+1)$$
$$\times \delta(\hbar\omega_c - \varepsilon(\tilde{m},\tilde{\imath})) \sum_{L'} (2L'+1) \begin{pmatrix} L & L' & \lambda \\ 0 & 0 & 0 \end{pmatrix}^2. \tag{100}$$

To carry out the summation over L', we utilize the following orthogonality relation for the Wigner-3j symbols [74]:

$$\sum_{j_3 m_3} (2j_3+1) \begin{pmatrix} j_1 & j_2 & j_3 \\ m_1 & m_2 & m_3 \end{pmatrix} \begin{pmatrix} j_1 & j_2 & j_3 \\ m_1' & m_2' & m_3 \end{pmatrix} = \delta_{m_1 m_1'} \delta_{m_2 m_2'}. \tag{101}$$

Considering values $2L \gg 1$, we can replace the L-sum by an integral and find

$$\gamma_{RP} = \frac{\hbar^4}{2\pi^2\mu^2\omega_c R^6} \iiint d\rho\, d\rho'\, dL^2(\rho\rho') \sqrt{\rho^2 - L^2}\sqrt{\rho'^2 - L^2}\, \delta(\hbar\omega_c - \varepsilon(\tilde{m},\tilde{\imath})). \tag{102}$$

From Eq. (102), one can see that the value of γ_{RP} is independent of λ for small $\lambda \ll k_F R$.

To proceed further, one first needs to execute the partial integration over ρ'. This is done by transforming the Dirac delta function as

$$\delta(\hbar\omega_c - \varepsilon(\tilde{m},\tilde{\imath})) = \frac{\mu R^2}{\hbar^2 \sqrt{\rho^2 - (k_F R)^2\zeta}}\, \delta(\rho' - \sqrt{\rho^2 - (k_F R)^2\zeta}), \tag{103}$$

where

$$\zeta = \hbar\omega_c/\varepsilon_F \tag{104}$$

and ε_F is the Fermi energy.

We first calculate γ_{RP} for the case $\zeta \leqslant 1$; we treat $\zeta > 1$ below. When $\zeta \leqslant 1$, integration over ρ' in (102) yields

$$\gamma_{RP} = \frac{\hbar k_F^4 R^2}{4\pi^2} \frac{2}{\zeta} \left[\int_0^{1-\zeta} dy \int_1^{1+\zeta} dz \sqrt{z-y}\sqrt{z-y-\zeta} \right.$$
$$\left. + \int_{1-\zeta}^{1} dy \int_{y+\zeta}^{1+\zeta} dz \sqrt{z-y}\sqrt{z-y-\zeta} \right], \qquad \zeta \leqslant 1, \tag{105}$$

where the dimensionless variables y and z are

$$y = (L/k_F R)^2, \qquad z = (\rho/k_F R)^2. \tag{106}$$

The integration limits in (105) have been determined to prevent both the delta function, $\delta(\hbar\omega_c - \varepsilon(\tilde{m},\tilde{\imath}))$, and the density (54) for the zeroes of a spherical Bessel function from vanishing.

The integrals in (105) can be evaluated by means of the three formulae in Ref. [75] and the formula in Ref. [76] to yield

$$\frac{\gamma_{RP}}{\gamma_{wf}} = g(\zeta) = \frac{(1+\zeta)^{3/2} - (1-\zeta)^{3/2}}{3\zeta} + \frac{\zeta}{4}\left[(1+\zeta)^{1/2} - (1-\zeta)^{1/2}\right] + \frac{\zeta}{4}\ln\left(\frac{2-\zeta+2\sqrt{1-\zeta}}{2+\zeta+2\sqrt{1+\zeta}}\right) - \frac{\zeta^2}{8}\ln\left[(2-\zeta+2\sqrt{1-\zeta})(2+\zeta+2\sqrt{1+\zeta})\right] + \frac{\zeta^2}{4}\ln\zeta, \qquad \zeta \leqslant 1. \tag{107}$$

In writing Eq. (107), we took into consideration the definition of γ_{wf} in Eq. (5). To facilitate the comparison, we notice that, in the case of a Fermi gas at zero temperature and with the definition (4) for the deformation parameter, the well-formula friction coefficient equals $\gamma_{wf} = \rho_\mu \bar{v} R^2 = (\hbar k_F^4 R^2)/(4\pi^2)$, when the spin degeneracy of the electrons is taken into account. The corresponding expression in Ref. [47] equals $\gamma_{wf} = (\hbar k_F^4 R^4)/(8\pi^2)$, since one kind of spin only was considered and the deformation parameter differed by a factor of R.

For large values of $\hbar\omega_c$ such that $\zeta > 1$, the integration of (102) by similar means yields

$$\frac{\gamma_{RP}}{\gamma_{wf}} = g(\zeta) = \frac{2}{\zeta}\int_0^1 dy \int_{y+\zeta}^{1+\zeta} dz \sqrt{z-y}\sqrt{z-y-\zeta} = \frac{1}{3\zeta}(1+\zeta)^{3/2} + \frac{\zeta}{4}(1+\zeta)^{1/2} - \frac{\zeta}{8}(\zeta+2)\ln\left[\frac{2+\zeta+2\sqrt{1+\zeta}}{\zeta}\right], \qquad \zeta > 1. \tag{108}$$

Appendix B

B.1.

Due to the central role played by expression (54) in determining the precise value of Landau damping, we show in detail in this appendix that it yields the correct volume term for the density of states in a spherical Fermi box. Indeed, expression (54) provides the density of zeroes of a spherical Bessel function $j_L(\rho)$ of given angular momentum L with respect to the argument ρ.

For fixed L, the total number S_L of the zeroes of $j_L(\rho)$ in the interval $0 < \rho \leqslant k_F R$ is given by the integral of (54), namely by

$$S_L = \int_L^{k_F R} \frac{dn}{d\rho}(L \text{ fixed})\, d\rho = \frac{1}{\pi}\int_L^{k_F R} \frac{d\rho}{\rho}\sqrt{\rho^2 - L^2}. \tag{109}$$

For given (L, M), S_L is also the number of radial wave functions that vanish at the boundary ($j_L(k_{Ln}R)=0$) and have wave numbers smaller than the Fermi wave number ($0<k_{Ln}\leqslant k_F$).

To calculate Eq. (109), we use the integral

$$\int \frac{dx}{x}\sqrt{x^2-a^2}=\sqrt{x^2-a^2}-a\arccos\left(\frac{a}{x}\right), \qquad a\geqslant 0, \tag{110}$$

and find that

$$S_L=\frac{1}{\pi}\left[\sqrt{(k_F R)^2-L^2}-L\arccos\left(\frac{L}{k_F R}\right)\right]. \tag{111}$$

The total number N of states with $k_{Ln}\leqslant k_F$ is given then by

$$\begin{aligned} N&=\sum_{L=0}^{k_F R}(2L+1)\,S_L \\ &\approx\int_0^{k_F R}\frac{2L\,dL}{\pi}\left[\sqrt{(k_F R)^2-L^2}-L\arccos\left(\frac{L}{k_F R}\right)\right]. \end{aligned} \tag{112}$$

To proceed further, one needs the following three integrals:

$$\int\sqrt{a^2-x}\,dx=-\frac{2}{3}(a^2-x)^{3/2}, \tag{113}$$

$$\int x^2\arccos\left(\frac{x}{a}\right)dx=\frac{x^3}{3}\arccos\left(\frac{x}{a}\right)+\frac{1}{3}\int\frac{x^3\,dx}{\sqrt{a^2-x^2}}, \tag{114}$$

$$\int\frac{x^3\,dx}{\sqrt{a^2-x^2}}=\frac{(a^2-x^2)^{3/2}}{3}-a^2\sqrt{a^2-x^2}. \tag{115}$$

With the help of Eqs. (113)–(115), one obtains

$$I_1=\frac{1}{\pi}\int_0^{k_F R}2L\,dL\sqrt{(k_F R)^2-L^2}=\frac{2}{3\pi}(k_F R)^3 \tag{116}$$

and

$$I_2=\frac{2}{\pi}\int_0^{k_F R}L^2\,dL\arccos\left(\frac{L}{k_F R}\right)=\frac{4}{9\pi}(k_F R)^3. \tag{117}$$

Therefore, the final result for the total number of states is

$$N=I_1-I_2=\frac{(k_F R)^3}{3\pi}\left[2-\frac{4}{3}\right]=\frac{2}{9\pi}(k_F R)^3=(\text{volume})\frac{k_F^3}{6\pi^2}. \tag{118}$$

As it ought to do, result (118) agrees exactly with the familiar result for the density of states for one kind of Fermi particles in a cubical box.

B.2.

Apart from the direct, but a posteriori, justification for the density (54) presented in the previous section there exist in the literature two a priori proofs based

(i) On expressions that yield the positions of zeroes of a usual Bessel function $J_\nu(\rho)$ when both the argument and the order are large [77, 78];

(ii) On the WKB quantization condition [79, 80].

In particular, for the (i) case here, the appropriate expression is [81]

$$J_\nu(\nu \sec \beta) = 0, \tag{119}$$

with

$$\nu(\tan \beta - \beta) + \chi = n\pi, \tag{120}$$

where χ here is a quantity varying very slowly with the order ν and remaining between the following limits for large ν:

$$\frac{\pi}{6} < \chi < \frac{\pi}{4}. \tag{121}$$

Naturally since $\rho = \nu \sec \beta$, the previous equations can be rearranged to yield

$$\rho \sin \beta - \beta\nu + \chi = n\pi. \tag{122}$$

For a spherical Bessel function, $\nu = L + \frac{1}{2}$, and differentiation of Eq. (122) with respect to dn, $d\rho$, and $d\beta$ immediately yields the density (54). Observe that we have neglected the $\frac{1}{2}$ in front of L for convenience. This is allowed because of the predominance of large L's. However, retaining this $\frac{1}{2}$ does not produce any changes.

Concerning case (ii), one needs to notice that, due to the separation of motion, the WKB quantization condition for a sphere yields the radial integral

$$\int_{(L+1/2)/k}^{R} \left\{ k^2 - \frac{(L+1/2)^2}{r^2} \right\}^{1/2} dr = n\pi - \frac{\pi}{4}. \tag{123}$$

Differentiation of (123) immediately yields the density (54). Note that even though the result is the same, the proof (i) based on the position of the zeroes of a Bessel function is more general than the WKB approach. Specifically, as an integration of Eq. (123) can show, the WKB quantization condition corresponds to Eq. (122) when χ is replaced by the upper limit $\pi/4$.

B.3.

In this subsection, we show that the McMahon formula for the location of the zeroes of a spherical Bessel function leads to an erroneous result when used to

calculate the volume term for the density of states in a spherical Fermi box. The total number N of states with $k_{Ln} \leqslant k_F$ is

$$N = \sum_{L=0}^{L_{max}} (2L+1) S_L, \tag{124}$$

where S_L is again the total number of zeroes of $j_L(\rho)$ in the interval $0 < \rho \leqslant k_F R$ for fixed L.

The McMahon formula for the location of the zeroes of a usual Bessel function $J_\nu(\rho)$ is given in Ref. [41]. According to this formula, the nth zero of the spherical $j_L(\rho)$, where

$$j_L(\rho) = \left(\frac{\pi}{2\rho}\right)^{1/2} J_{L+1/2}(\rho), \tag{125}$$

is located at $z_{L,n}$ given by

$$z_{L,n} = \left[\beta - \frac{L(L+1)}{2\beta} + \cdots\right], \qquad \text{where} \quad \beta = \pi\left(n + \frac{L}{2}\right). \tag{126}$$

Then setting $z_{L,n} = k_F R$ gives an estimate of $S_L = n$ via

$$k_F R = \pi S_L + L\pi/2. \tag{127}$$

Whence,

$$\begin{aligned} N &= \sum_{L=0}^{L_{max}} (2L+1)\left[\frac{k_F R}{\pi} - \frac{L}{2}\right] \\ &\approx \left[\frac{k_F R}{\pi} \int_0^{L_{max} = 2k_F R/\pi} 2L\, dL\right] - \int_0^{2k_F R/\pi} L^2\, dL \\ &= \left(\frac{k_F R}{\pi}\right)^3 \left(4 - \frac{8}{3}\right) = (\text{volume}) \frac{k_F^3}{\pi^4}. \end{aligned} \tag{128}$$

Result (128) does not agree with the correct result for a cubical box, namely, with $k_F^3/6\pi^2$; specifically, it underestimates the total number of states by a factor of $6/\pi^2$.

REFERENCES

1. W. A. DE HEER, K. SELBY, V. KRESIN, J. MASUI, M. VOLLMER, A. CHÂTELAIN, AND W. D. KNIGHT, *Phys. Rev. Lett.* **59** (1987), 1805.
2. K. SELBY, M. VOLLMER, J. MASUI, V. KRESIN, W. A. DE HEER, AND W. D. KNIGHT, *Phys. Rev. B* **40** (1989), 5417.
3. K. SELBY, V. KRESIN, J. MASUI, M. VOLLMER, W. A. DE HEER, A. SCHEIDEMANN, AND W. D. KNIGHT, *Phys. Rev. B* **43** (1991), 4565; K. SELBY, Ph.D. thesis, University of California, Berkeley, 1990.

4. C. BRÉCHIGNAC, PH. CAHUZAC, F. CARLIER, AND J. LEYGNIER, *Chem. Phys. Lett.* **164** (1989), 433.
5. C. R. C. WANG, S. POLLACK, D. CAMERON, AND M. M. KAPPES, *J. Chem. Phys.* **93** (1990), 3787; C. R. C. WANG, S. POLLACK, AND M. M. KAPPES, *Chem. Phys. Lett.* **166** (1990), 26.
6. S. POLLACK, C. R. C. WANG, AND M. M. KAPPES, *J. Chem. Phys.* **94** (1991), 2496.
7. H. FALLGREN AND T. P. MARTIN, *Chem. Phys. Let.* **168** (1990), 233.
8. W. EKARDT, *Phys. Rev. B* **31** (1985), 6360; W. EKARDT AND Z. PENZAR, *Phys. Rev. B* **43** (1991), 1322.
9. D. E. BECK, *Phys. Rev. B* **35** (1987), 7325.
10. C. YANNOULEAS, R. A. BROGLIA, M. BRACK, AND P.-F. BORTIGNON, *Phys. Rev. Lett.* **63** (1989), 255.
11. C. YANNOULEAS, J. M. PACHECO, AND R. A. BROGLIA, *Phys. Rev. B* **41** (1990), 6088.
12. V. KRESIN, *Phys. Rev. B* **42** (1990), 3247.
13. M. BRACK, *Phys. Rev. B* **39** (1989), 3533.
14. EL. SERRA, F. GARCÍAS, M. BARRANCO, J. NAVARRO, L. C. BALBÁS, AND A. MAÑANES, *Phys. Rev. B* **39** (1989), 8247.
15. E. LIPPARINI AND S. STRINGARI, *Z. Phys. D* **18** (1991), 193.
16. G. F. BERTSCH, *Comput. Phys. Commun.* **60** (1990), 247.
17. J. M. PACHECO AND R. A. BROGLIA, *Phys. Rev. Lett.* **62** (1989), 1400.
18. G. F. BERSCH AND D. TOMÁNEK, *Phys. Rev. B* **40** (1989), 2749.
19. V. BONAČIĆ-KOUTECKÝ, M. M. KAPPES, P. FANTUCCI, AND J. KOUTECKÝ, *Chem. Phys. Lett.* **170** (1990), 26; V. BONAČIĆ-KOUTECKÝ, P. FANTUCCI, AND J. KOUTECKÝ, *J. Chem. Phys.* **93** (1990), 3802.
20. C. YANNOULEAS AND R. A. BROGLIA, *Phys. Rev. A* **44** (1991), 5793.
21. J. M. PACHECO, R. A. BROGLIA, AND B. R. MOTTELSON, "The Intrinsic Line Width of the Plasmon Resonances in Metal Microclusters at Very Low Temperatures: Quantal Surface Fluctuations," Preprint NBI-90-44.
22. R. A. BROGLIA, J. M. PACHECO, AND C. YANNOULEAS, *Phys. Rev. B* **44** (1991), 5901.
23. G. MIE, *Ann. Phys. (Leipzig)* **25** (1908), 377.
24. R. H. DOREMUS, *J. Chem. Phys.* **40** (1964), 2389; **42** (1965), 414.
25. U. KREIBIG, *J. Phys. F* **4** (1974), 999.
26. L. GENZEL, T. P. MARTIN, AND U. KREIBIG, *Z. Phys. B* **21** (1975), 339.
27. M. A. SMITHARD, *Solid State Commun.* **14** (1974), 407.
28. K.-P. CHARLÉ, F. FRANK, AND W. SCHULZE, *Ber. Bunsen-Ges. Phys. Chem.* **88** (1984), 350.
29. For a review, cf. U. KREIBIG AND L. GENZEL, *Surf. Sci.* **156** (1985), 678.
30. For a review, cf. W. P. HALPERIN, *Rev. Mod. Phys.* **58** (1986), 533.
31. A. KAWABATA AND R. KUBO, *J. Phys. Soc. Jpn.* **21** (1966), 1765.
32. L. SANDER, *J. Phys. Chem. Solids* **29** (1968), 291.
33. M. CINI AND P. ASCARELLI, *J. Phys. F* **4** (1974), 1998.
34. R. RUPPIN AND H. YATOM, *Phys. Status Solidi B* **74** (1976), 647.
35. A. A. LUSHNIKOV AND A. J. SIMONOV, *Z. Phys.* **270** (1974), 17.
36. D. B. TRAN THOAI AND W. EKARDT, *Solid State Commun.* **41** (1982), 687.
37. D. M. WOOD AND N. W. ASHCROFT, *Phys. Rev. B* **25** (1982), 6255.
38. W. A. KRAUS AND G. C. SCHATZ, *J. Chem. Phys.* **79** (1983), 6130.
39. H. GÖHLICH, T. LANGE, T. BERGMANN, AND T. P. MARTIN, *Phys. Rev. Lett.* **65** (1990), 748.
40. S. BJØRNHOLM, J. BORGGREEN, O. ECHT, K. HANSEN, J. PEDERSEN, AND H. D. RASMUSSEN, *Phys. Rev. Lett.* **65** (1990), 1627.
41. M. ABRAMOWITZ AND I. A. SEGUN, "Handbook of Mathematical Functions," No. 9.5.12, Dover, New York, 1968.
42. J. EULER, *Z. Phys.* **137** (1954), 318.
43. J. BLOCKI, Y. BONEH, J. R. NIX, J. RANDRUP, M. ROBEL, A. J. SIERK, AND W. J. SWIATECKI, *Ann. Phys. (N.Y.)* **113** (1978), 330.
44. J. RANDRUP, *Nucl. Phys. A* **383** (1982), 468.
45. W. U. SCHRÖDER AND J. R. HUIZENGA, *in* "Treatise on Heavy-Ion Science" (D. A. Bromley, Ed.), Vol. 2, Plenum, New York, 1985.

46. YU. TS. OGANESSIAN AND YU. A. LAZAREV, *in* "Treatise on Heavy-Ion Science" (D. A. Bromley, Ed.), Vol. 4, Plenum, New York, 1985.
47. C. YANNOULEAS, *Nucl. Phys. A* **439** (1985), 336.
48. G. BERTSCH AND H. ESBENSEN, *Phys. Lett. B* **161** (1985), 248.
49. C. YANNOULEAS, *Nucl. Phys. A* **489** (1988), 91.
50. J. R. NIX AND A. J. SIERK, *Phys. Rev. C* **21** (1980), 396.
51. Å. BOHR AND B. R. MOTTELSON, "Nuclear Struture," Vol. II, Benjamin, Reading, MA, 1975.
52. D. J. ROWE, "Nuclear Collective Motion," Methuen, London, 1970.
53. G. E. BROWN, "Unified Theory of Nuclear Models and Forces," 2nd ed., North-Holland, Amsterdam, 1967.
54. N. D. LANG AND W. KOHN, *Phys. Rev. B* **3** (1971), 1215; N. D. LANG, *Solid State Phys.* **28** (1970), 225, and references therein.
55. C. YANNOULEAS, M. DWORZECKA, AND J. J. GRIFFIN, *Nucl. Phys. A* **379** (1982), 256.
56. U. FANO, *Phys. Rev.* **124** (1961), 1866.
57. L. D. LANDAU, *J. Phys. USSR* **10** (1946), 25.
58. A. L. FETTER AND J. D. WALECKA, "Quantum Theory of Many-Body Particle Systems," Section 34, McGraw–Hill, New York, 1979.
59. D. PINES, "Elementary Excitations in Solids," Benjamin, New York, 1964.
60. C. YANNOULEAS, M. DWORZECKA, AND J. J. GRIFFIN, *Nucl. Phys. A* **397** (1983), 239.
61. W. EKARDT, *Phys. Rev. B* **29** (1984), 1558.
62. J. M. BLATT AND V. F. WEISSKOPF, "Theoretical Nuclear Physics," Chap. VIII.9.A, Springer-Verlag, New York, 1979.
63. M. J. PUSKA, R. M. NIEMINEN, AND M. MANNINEN, *Phys. Rev.* **31** (1985), 3486 (in particular, Fig. 3 and subsequent discussion).
64. R. BALIAN AND C. BLOCH, *Ann. Phys (N.Y.)* **60** (1970), 401.
65. M. ACHÈCHE *et al.*, *Ultramicroscopy* **20** (1986), 99.
66. C. YANNOULEAS, M. DWORZECKA, AND J. J. GRIFFIN, *Nucl. Phys. A* **339** (1980), 219.
67. R. KUBO, "Statistical Mechanics," North-Holland, Amsterdam, 1965.
68. Å. BOHR AND B. R. MOTTELSON, "Nuclear Structure," Vol. I, App. 2D, Benjamin, Reading, MA, 1969.
69. W. A. SAUNDERS, *Phys. Rev. Lett.* **64** (1990), 3046.
70. M. NAKAMURA, Y. ISHII, A. TAMURA, AND S. SUGANO, *Phys. Rev. A* **42** (1990), 2267.
71. E. LIPPARINI AND A. VITTURI, *Z. Phys. D* **17** (1990), 57.
72. F. GARCÍAS, J. A. ALONSO, AND J. M. LÓPEZ, *Phys. Rev. B* **43** (1991), 9459.
73. G. B. ARFKEN, "Mathematical Methods for Physicists," Nos. 11.170, 11.162, Academic Press, New York, 1970.
74. A. R. EDMONDS, "Angular Momentum in Quantum Mechanics," pp. 63, 47, Princeton Univ. Press, Princeton, NJ, 1957.
75. I. S. GRADSHTEYN AND I. W. RYZHIK, "Tables of Integrals, Series, and Products," Nos. 2.275.3, 2.831, 2.272.7, Academic Press, New York, 1965.
76. W. GRÖBNER AND N. HOFREITER, "Integraltafel," Vol. I, p. 116, No. 323.23b, Springer-Verlag, Vienna, 1975.
77. R. M. MAZO, *Am. J. Phys.* **28** (1960), 332.
78. R. H. LAMBERT, *Am. J. Phys.* **36** (1968), 417.
79. W. PAULI, "Handbuch der Physik" (S. Flügge, Ed.), Vol. 5, p. 92, Springer-Verlag, Berlin, 1958.
80. E. A. POWER, "Introductory Quantum Electrodynamics," Longmans Green & Co., London, 1964.
81. G. N. WATSON, "Treatise on the Thry of Bessel Functions," pp. 514, 515, Cambridge Univ. Press, New York, 1952.